Annu. Rev. Astron. Astrophys. 1997. 35:179–215

DENSE PHOTODISSOCIATION REGIONS (PDRs)[1]

D. J. Hollenbach and A. G. G. M. Tielens
MS 245-3, NASA Ames Research Center, Moffett Field, California 94035;
e-mail: hollenbach@warped.arc.nasa.gov, tielens@dusty.arc.nasa.gov

KEY WORDS: interstellar medium, astrochemistry, infrared astronomy, nebulae, atomic processes

ABSTRACT

All neutral atomic hydrogen gas and a large fraction of the molecular gas in the Milky Way Galaxy and external galaxies lie in PDRs, and PDRs are the origin of most of the nonstellar infrared (IR) and the millimeter CO emission from a galaxy. On the surfaces ($A_v < 1-3$) of interstellar clouds, the absorption of far ultraviolet (FUV) photons ($h\nu < 13.6$ eV) by gas and dust grains leads to intense emission of [C II] 158 μm, [O I] 63, 146 μm, and H_2 rovibrational transitions, as well as IR dust continuum and polycyclic aromatic hydrocarbon (PAH) emission features. Deeper in PDRs, CO rotational and [C I] 370, 609 μm lines originate. The transition of H to H_2 and C^+ to CO occurs within PDRs. Theoretical models compared with observations diagnose such physical parameters as the density and temperature structure, the elemental abundances, and the FUV radiation field in PDRs. Applications include clouds next to H II regions, reflection nebulae, planetary nebulae, red giant outflows, circumstellar gas around young stars, diffuse clouds, the warm neutral medium (WNM), and molecular clouds in the interstellar radiation field: in summary, much of the interstellar medium in galaxies. This review focuses on dense PDRs in the Milky Way Galaxy. Theoretical PDR models help explain the observed correlation of the CO J = 1–0 luminosity with the molecular mass and also suggest FUV-induced feedback mechanisms that may regulate star formation rates and the column density through giant molecular clouds.

1. INTRODUCTION

The study of photodissociation regions (PDRs, also called photon-dominated regions) is the study of the importance of FUV (6 eV $< h\nu <$ 13.6 eV) photons on the structure, chemistry, thermal balance, and evolution of the neutral interstellar medium of galaxies. One important aspect of this study is understanding the process of star formation. FUV photons not only illuminate star-forming regions, causing them to glow in infrared (IR) emission diagnostic of the physical conditions, but they also may play an important role regulating the star formation process itself in a galaxy.

Historically, the study of PDRs was stimulated by the early observations of the massive star-forming regions Orion A and M17 in the fine structure lines [C II] 158 μm and [O I] 63 μm by Melnick et al (1979), Storey et al (1979), and Russell et al (1980, 1981). These observations pointed to predominantly neutral IR-luminous regions lying outside H II regions. These PDRs are photodissociated and, for elements like carbon with ionization potentials below 13.6 eV, photoionized by the FUV fluxes generated by nearby O stars. The luminosity in the [C II] and [O I] lines, which dominate the cooling of the atomic gas, is on the order of 10^{-3}–10^{-2} of the IR luminosity from the dust that absorbed the starlight. Figure 1 shows a more recent map of the [C II] 158 μm and [O I] 63 μm emission from Orion A (Herrmann et al 1997), showing the large extent ($\gtrsim 5'$ by $5'$ or 0.75 pc by 0.75 pc) and luminosity ($L_{CII} \sim 80\ L_\odot$ and $L_{OI} \sim 600\ L_\odot$) of the IR-glowing neutral gas associated with the Trapezium stars. Figure 2 (Tielens et al 1993) shows a smaller scale map of the Orion Bar, where the neutral gas outside of the H II region is viewed edge-on. A layered appearance is evident; moving away from the excitation source, the ionization front, H I layer, H_2 emission, and CO emission appear in succession.

Despite its historical roots, the study of PDRs is not simply the study of photodissociated gas that lies just outside of dense, luminous H II regions in the Galaxy; it includes as well the pervasive warm neutral medium (WNM), diffuse and translucent clouds, reflection nebulae, the neutral gas around planetary nebulae, photodissociated winds from red giant and asymptotic giant branch (AGB) stars, and the interstellar medium (ISM) in the nuclei of starburst galaxies and galaxies with active galactic nuclei (AGNs). PDRs include all interstellar regions where the gas is predominantly neutral but where FUV photons play a significant role in the chemistry and/or the heating. Figure 3 schematically illustrates the structure of a PDR. The ultraviolet flux from, for example, the interstellar radiation field (ISRF) or from nearby hot stars is incident on a neutral cloud of hydrogen nucleus density n. The incident FUV flux G_0 (in units of an average interstellar flux of 1.6×10^{-3} erg cm^{-2} s^{-1}; Habing 1968) can range from the local average ISRF ($G_0 \sim 1.7$, Draine 1978) to $G_0 \gtrsim 10^6$, appropriate,

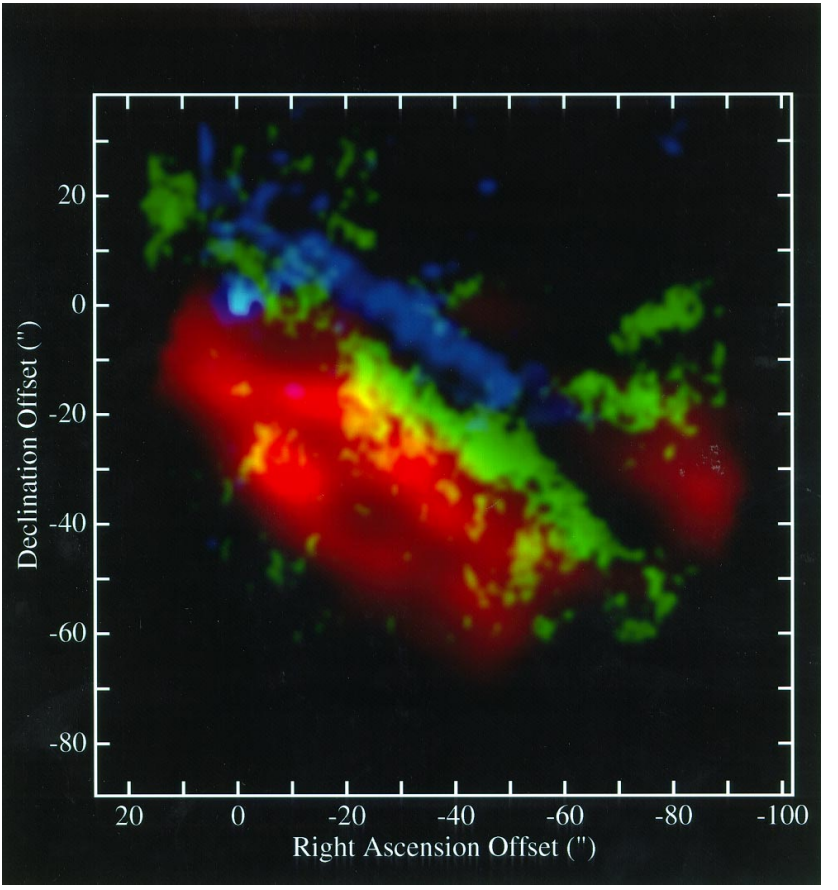

Figure 2 The Orion Bar region mapped in the 3.3-μm PAH feature *(blue)*, H_2 1-0 S(1) emission *(yellow)*, and CO J=1-0 emission *(red;* Tielens et al 1993). The (0,0) position corresponds to the (unrelated) star θ^2 A Ori. The illuminating source, θ^1 C Ori and the ionized gas are located to the northwest. For all three tracers, the emission is concentrated in a bar parallel to but displaced to the southeast from the ionization front. The PDR is seen edge on; a separation of $\simeq$ 10" is seen between the PAH emission and the H_2 emission, as well as between the H_2 emission and the CO emission, as predicted by PDR models (see text).

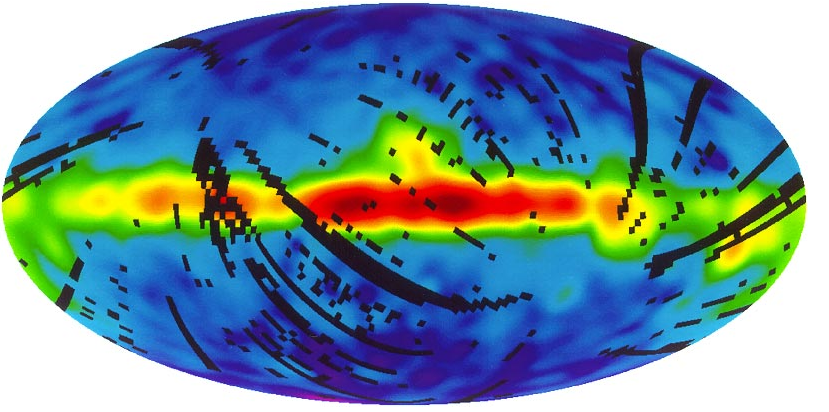

Figure 4 The [CII] emission of the galaxy observed by the FIRAS instrument on COBE (Bennett et al 1994) (158-μm C^+ line intensity). The galactic plane is horizontal with the galactic center at the center.

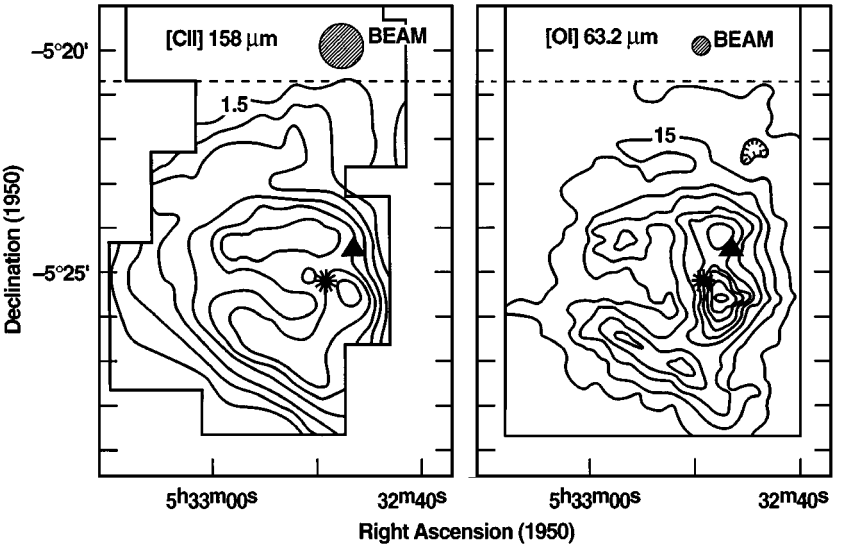

Figure 1 [C II] 158 μm and [O I] 63 μm maps of the Orion A molecular cloud behind the Trapezium (adapted from Herrmann et al 1997). The [C II] contours are in steps of 5×10^{-4} erg cm^{-2} s^{-1} sr^{-1} beginning with 1.5×10^{-3} erg cm^{-2} s^{-1} sr^{-1}. The [O I] are in steps of 10×10^{-3} erg cm^{-2} s^{-1} sr^{-1} beginning with 15×10^{-3} erg cm^{-2} s^{-1} sr^{-1}. A small area of $\simeq 1'$ ($\simeq$0.15 pc) around IRc 2 has significant [O I] shock emission. The asterisk and triangle indicate the location of θ^1 C Ori and IRc 2, respectively.

for example, to gas closer than 0.1 pc from an O star. Typically, densities n range from $\sim$0.25 cm^{-3} in the WNM, to $\sim$10–100 cm^{-3} in diffuse clouds, to $\sim 10^3$–10^7 cm^{-3} in the PDRs associated with molecular gas. As illustrated in Figure 3, PDRs are often overlaid with H II gas and a thin H II/H I interface that absorb the Lyman continuum photons. Although dependent on the ratio G_0/n, the PDR itself is often characterized by a layer of atomic hydrogen that extends to a depth $A_v \sim 1$–2 (or a hydrogen nucleus column of $N = 2$–4×10^{21} cm^{-2}) from the ionization front, a layer of C^+ that extends to a depth $A_v \sim 2$–4, and a layer of atomic oxygen that extends to a depth $A_v \sim 10$. The H, C^+, and O layers are maintained by the FUV photodissociation of molecules and the FUV photoionization of carbon.

Traditionally, PDRs have been associated with atomic gas. However, with the above definition, PDRs include material in which the hydrogen is molecular and the carbon is mostly in CO, but where FUV flux still strongly affects the chemistry of oxygen and carbon not locked in CO (photodissociating OH, O_2, and H_2O, for example) and the ionization fraction. With the exception of the

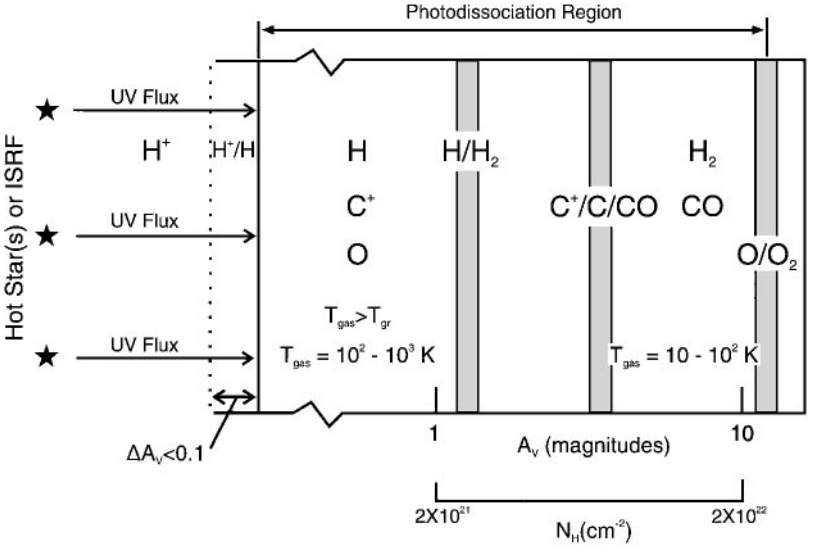

Figure 3 A schematic diagram of a photodissociation region. The PDR is illuminated from the left and extends from the predominantly atomic surface region to the point where O_2 is not appreciably photodissociated ($\simeq$10 visual magnitude). Hence, the PDR includes gas whose hydrogen is mainly H_2 and whose carbon is mostly CO. Large columns of warm O, C, C^+, and CO and vibrationally excited H_2 are produced in the PDR. The gas temperature T_{gas} generally exceeds the dust temperature T_{gr} in the surface layer.

molecular gas in dense star-forming cores, most molecular gas in the Galaxy is found at $A_v \lesssim 10$ in Giant Molecular Clouds (GMCs). Therefore, *all of the atomic and most of the molecular gas in the Galaxy is in PDRs.*

Not only do PDRs include most of the mass of the ISM, but PDRs are the origin of much of the IR radiation from the ISM (the other significant sources are H II regions and dust heated by late-type stars). The incident starlight is absorbed primarily by large carbon molecules (polycyclic aromatic hydrocarbons or PAHs) and grains inside a depth $A_v \sim 1$. Most of the absorbed energy is used to excite the PAHs and heat the grains and is converted to PAH IR features and far-infrared (FIR) continuum radiation of the cooling grains. However, typically 0.1–1% of the absorbed FUV energy is converted to energetic ($\sim$1 eV) photoelectrons that are ejected from PAHs and grains and heat the gas ("photoelectric heating"). Although the gas receives 10^2–10^3 times less heating energy per unit volume than the dust, the gas attains higher equilibrium temperatures because of the much less efficient cooling of the gas (via [C II] 158 μm and [O I] 63 μm) relative to the radiative dust cooling.

Much of the [C II], [O I], and [Si II] fine-structure, carbon recombination, the H_2 rotational and vibrational, and C I(9850 Å) emission in galaxies originates from depths $A_v \lesssim 4$ in PDRs. Most of the [C I] fine structure and the CO rotational emission in galaxies comes from regions somewhat deeper in PDRs. For example, the COBE 4-μm to 1000-μm spectrum of our Milky Way Galaxy (Wright et al 1991) is dominated by PDR emission (see Figure 4 for the [C II] map), with the exception of the [N II] and a fraction of the [C II] fine structure emission, which originates in diffuse H II gas. Evident in Figure 4 are the PDRs associated with the the molecular ring at 3 kpc and the GMCs in Ophiuchus and Orion.

We discuss the physical and chemical processes in PDRs in Section 2, followed by a summary of the theoretical models in Section 3. The observations of dense PDRs in the Milky Way Galaxy (Section 4) span a wide variety of phenomena and diagnose the physical conditions in neutral gas around H II regions, reflection nebulae, planetary nebulae, and the Galactic Center. PDR models explain the H_2 spectra, the origin of [C I], the correlation of [C II] to CO J = 1–0, and the correlation of ([C II] + [O I]) to the IR continuum intensity (Section 4). We conclude in Section 5 with brief descriptions of PDR models applied to some interesting problems, including the scaling of CO luminosity with mass, the effect of X rays on molecular gas (X-ray dissociation regions or XDRs), the interstellar conditions of the starburst nucleus of M82, and the regulation of star formation.

Because of space limitations in this review, we have focused on dense PDRs in our Galaxy. Hollenbach & Tielens (1996) present a more comprehensive PDR review that discusses global models of the ISM of the Milky Way and other galaxies, the distribution of H I and H_2 in galaxies, H I halos around molecular clouds, the formation of molecular clouds, diffuse and translucent clouds, the neutral phases of the ISM, and more detailed discussion of the problems summarized in Section 5. Glassgold (1996) reviews PDRs associated with red giant outflows. Other PDR reviews include Genzel et al (1989), Jaffe & Howe (1989), Hollenbach (1990), Genzel (1991, 1992), Burton (1992), Sternberg (1992), van Dishoeck (1992), Hollenbach & Tielens (1996), and Sternberg et al (1997).

2. PHYSICAL AND CHEMICAL PROCESSES

2.1 *The Penetration of FUV Radiation*

One of the keys to understanding PDR structure lies in understanding the attenuation of FUV continuum flux through the PDR. The penetration of FUV radiation is determined by dust absorption and scattering and the geometry and

global structure of interstellar clouds. Various authors have studied the penetration of FUV radiation inside homogeneous clouds. In particular, Roberge et al (1981, 1991) solved the radiative transfer equation for plane parallel slabs of various thicknesses and calculated photodissociation and photoionization rates for a variety of astrophysically relevant molecules. Deep inside semi-infinite slabs, the mean intensity is proportional to $\exp[-kA_v]$, where k is a scale factor and A_v the visual extinction measured from the surface. For optically thin clouds, a correction has to be included for photons penetrating from the other side of the slab. Generally, a biexponential fit to the radiative transfer solution suffices (van Dishoeck 1988, Roberge et al 1991).

The intensity of the radiation field inside interstellar clouds depends critically on the adopted absorption and scattering properties of the dust. Generally, theoretical studies rely on either directly measured "average" properties of interstellar dust (cf Savage & Mathis 1979, Mathis 1990) or on models that fit these "average" properties (e.g. Draine & Lee 1984). These "average" dust properties refer exclusively to a (very biased) sample of lines of sight through diffuse interstellar clouds. Moreover, the dust properties are known to vary from one diffuse cloud to another (cf Cardelli et al 1989). Finally, dust in molecular clouds is generally characterized by a high value for R, the ratio of total to selective extinction. If diffuse clouds are a guide, this implies much lower FUV extinction per hydrogen atom than commonly adopted. The uncertainty can easily amount to 50% in k.

In recent years, it has become increasingly clear that interstellar clouds are inhomogeneous on all scales (e.g. Falgarone & Phillips 1996 and references therein). This clumpy nature of interstellar clouds can have a profound influence on the penetration of FUV radiation (Stutzki et al 1988, Boissé 1990, Spaans 1996, Hegmann & Kegel 1996). The study by Boissé is particularly instructive and establishes simple scaling laws that can be easily adopted for PDR modeling (cf Tauber & Goldsmith 1990, Howe et al 1991, Hobson & Scheuer 1994, Meixner & Tielens 1993). Depending on the clump filling factor and the density contrast between clump and interclump gas, the scale size for the penetration of FUV radiation can vary by orders of magnitude.

One important characteristic of FUV penetration into clumpy clouds is the existence of large fluctuations in the mean intensity at a given depth (Boissé 1990, Spaans 1996). These fluctuations are particularly important when individual clumps are optically thick (optical depth τ_0), scattering in the clump or interclump gas is unimportant, and the cloud is illuminated by a unidirectional field (i.e. a nearby star). In this limit, the FUV field can fluctuate by $\sim\exp(\tau_0)$ (Monteiro 1991, Störzer et al 1997). When any of these restrictions are relaxed, fluctuations become of lesser importance and may be no more than a factor of a few in realistic situations (Boissé 1990).

2.2 *Chemistry in PDRs*

PDR chemistry has been discussed in detail by Tielens & Hollenbach (1985a,c), LeBourlot et al (1993), Hollenbach et al (1991), Fuente et al (1993, 1995), Jansen et al (1995a,b), and Sternberg & Dalgarno (1995). It derives rather directly from the chemistry of those more transparent PDRs, diffuse and translucent clouds (Glassgold & Langer 1974, 1976, Black & Dalgarno 1976, Federman et al 1980, 1984, 1994, Danks et al 1984, van Dishoeck & Black 1986, 1988, 1989, Viala 1986, Viala et al 1988, Federman & Huntress 1989, van Dishoeck 1991, Heck et al 1992, Turner 1996, and references therein). PDR chemistry differs from normal ion-molecule chemistry in a number of ways. Obviously, because of the high FUV flux, photoreactions are very important, as are reactions with atomic hydrogen. Likewise, vibrationally excited H_2 is abundant and can play a decisive role in PDR chemistry. If the gas gets very warm ($\gtrsim$500 K), the activation barrier of reactions of atoms and radicals with H_2 can be easily overcome and these types of reactions can dominate. Electron recombination and charge exchange reactions are important for the ionization balance. Finally, the FUV flux keeps atomic O very abundant throughout the PDR, and hence burning reactions are effective. Here, we first discuss H_2 and CO self-shielding. We follow this with a discussion of the chemistry that can occur when the reactants have non-Maxwellian excitation of the vibrational or translational degrees of freedom. Finally, we briefly summarize chemical networks for PDRs.

PHOTODISSOCIATION AND SELF-SHIELDING OF H_2 AND CO Photodissociation and self-shielding of H_2 has been discussed by Field et al (1966), Stecher & Williams (1967), Hollenbach et al (1971), Jura (1974), Black & Dalgarno (1977), Shull (1978), Federman et al (1979), deJong et al (1980), van Dishoeck & Black (1986), Abgrall et al (1992), Heck et al (1992), LeBourlot et al (1993), and Lee et al (1996); reviewed by van Dishoeck (1987); and recently studied in detail by Draine & Bertoldi (1996), so a short summary will suffice here. Photodissociation of H_2 proceeds through FUV absorption in the Lyman and Werner transitions in the 912- to 1100-Å range, followed by fluorescence to the vibrational continuum of the ground electronic state about 10–15% of the time (see Figure 6 in Section 2.4). The H_2 photodissociation rate follows then from a summation over all lines. When the H_2 column density exceeds 10^{14} cm^{-2}, the FUV absorption lines become optically thick and self-shielding becomes important. The photodissociation rate then depends on the H_2 abundance and level population distribution as a function of depth in the cloud. Various approximations, appropriate for chemical modeling, have been described by Jura (1974), Federman et al (1979), van Dishoeck & Black (1986), and Draine & Bertoldi (1996). Self-shielding alone dominates H_2 dissociation and hence the

location of the H/H_2 transition when $G_0/n \lesssim 0.01$–0.1 cm^3. This includes diffuse clouds exposed to the interstellar radiation field and dense clumps in PDRs with higher FUV fluxes. Because of the self-shielding, the H_2 column increases rapidly and the H/H_2 transition zone is quite sharp. PDRs associated with bright FUV sources typically have $G_0/n \sim 1$ cm^3. The location of the H/H_2 transition is then dominated by dust absorption and typically occurs at $A_v \simeq 2$. At that point, dust has reduced the H_2 photodissociation rate sufficiently that an appreciable column of H_2 can build up, H_2 self-shielding takes over, and the H/H_2 transition will be very rapid again.

Photodissociation of CO has been studied in detail by Bally & Langer (1982), Glassgold et al (1985), van Dishoeck & Black (1988), Viala et al (1988), and Lee et al (1996). High-resolution laboratory studies show that CO photodissociation occurs through discrete absorption into predissociating bound states, implying that CO is also affected by self-shielding (Eidelsberg et al 1992). Further complications arise because of line coincidence with H and H_2. CO shielding functions have been tabulated by van Dishoeck & Black (1988) and by Lee et al (1996). For low ratios of G_0/n, the effects of CO self-shielding can lead to isotopic fractionation effects at the borders of clouds, where the rarer CO isotopes are preferentially photodissociated. The location of the C^+/C/CO transition in bright PDRs is largely governed by dust extinction. Because of the much lower abundance of CO relative to H_2, the CO rarely builds up sufficient column to self-shield in the $A_v \lesssim 1$ layer and the C^+/C/CO transition is much less sharp than that of H/H_2. Like H_2, CO abundances can be appreciable near the surfaces of dense clumps. However, that is not a result of self-shielding but rather reflects the high H_2 abundance near the surfaces of such clumps, which leads to an enhanced CO formation rate.

NON-MAXWELLIAN CHEMISTRY Neutral-neutral reactions are often endothermic and/or possess appreciable activation barriers because bonds have to be broken or rearranged. In PDRs, reactions of molecular hydrogen with C^+, O, N, S^+, and Si^+ are particularly important in initiating the chemical reactions. FUV pumping of H_2 can lead to a vibrational excitation temperature that is considerably higher than the gas temperature. Reactions with vibrational hot H_2 (H_2^*) have been discussed in an astrophysical context by Wagner & Graff (1987). Non–equilibrium excitation conditions can give rise to reaction rates that are considerably enhanced over the thermal ones (Gardiner 1977, Dalgarno 1985). For example, studies of the $O + H_2^*$, $OH + H_2^*$, and $C^+ + H_2^*$ reactions show large enhancements with vibrational excitation of H_2 (Light 1978, Schinke & Lester 1979, Schatz & Elgersma 1980, Schatz 1981, Schatz et al 1981, Lee et al 1982, Jones et al 1986). However, state-to-state chemistry is very selective and vibrational excitation of OH does not enhance the reaction rate of $OH + H_2$.

For lack of better knowledge, most studies of the chemistry in PDRs generally assume that exothermic reactions with H_2^* occur at the collision rate.

Translational energy can also be effective in promoting chemical reactions. In particular, the presence of turbulence can lead to non-Maxwellian velocity fields and, hence, non-Maxwellian reaction rates. This effect in PDRs has been shown to be important by Spaans et al (1997) for the reaction $C^+ + H_2$, which is endothermic by 0.4 eV. Because of their larger activation barriers, the reactions $O + H_2$ and $N + H_2$ are much less affected. Spaans & Jansen (in preparation; see Spaans 1995) evaluated in a simplified way, using estimated reaction rates, the effects of turbulence on sulfur chemistry. Finally, Falgarone et al (1995) examined the enhancement of OH, H_2O, CH^+, and HCO^+ in turbulent PDRs.

PDR CHEMICAL NETWORKS The most important reactions in the chemistry of carbon and oxygen compounds are schematically shown in Figure 5. Figure 5 is adapted from Sternberg & Dalgarno (1995) who provide a detailed discussion of PDR chemistry. The PDR surface layer consists largely of neutral or cationic atoms created by photodissociation and ionization reactions. Oxygen-bearing radicals (i.e. OH) are built up through reactions of O with H_2^* and H_2. Most of the OH produced is photodissociated again, but a small fraction reacts with

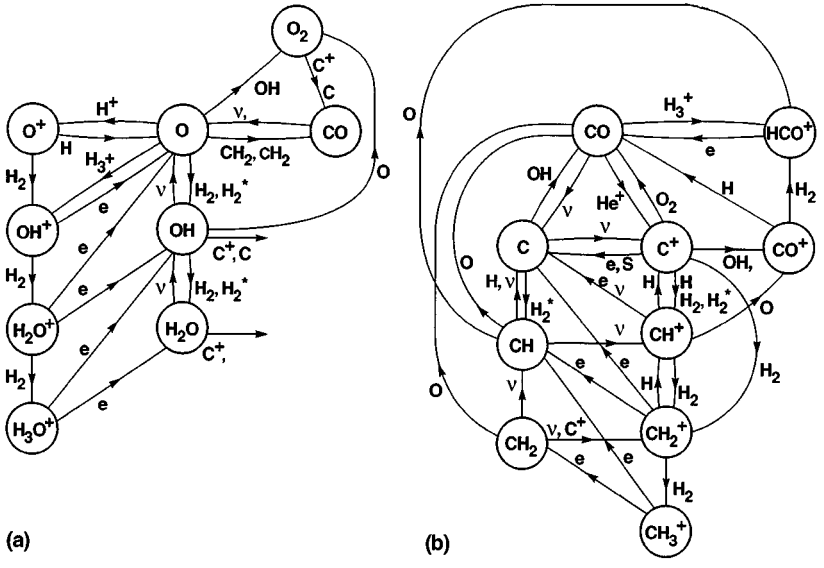

Figure 5 The most important reactions involved in the PDR chemistry of oxygen-bearing (*left*) and carbon-bearing (*right*) compounds (adapted from Sternberg & Dalgarno 1995).

C^+ to form CO^+, which charge exchanges with H to form CO. Some CO^+ is also formed through the reaction of CH^+ with O ("burning"). The CO photodissociates again. The C^+/C balance is dominated by photoionization and radiative recombination reactions. A small fraction of the C^+ reacts with H and H_2^* to form CH^+. Likewise, a small fraction of the neutral C flows to CH through reaction with H_2^*. Through reactions with H, CH^+ and CH reform C^+ and C, respectively. Photoreactions are important for C, OH, and CO but not for the small hydrocarbon radicals and cations. With increasing depth in this so-called radical zone (but recall it is largely atomic), the chemistry involving small radicals, such as the CH_n^+-family and OH, becomes more important. In cool low-density PDRs, reactions with FUV-pumped vibrationally excited H_2^* are important, whereas in warm high-density PDRs, reactions with H_2 dominate. In this case, reactions of C^+ with H_2 followed by dissociative electron recombination of CH^+ to C can be an important recombination route for C^+. As the depth increases, CO formation by burning of small neutral radicals (i.e. CH, CH_2) becomes more important than the OH-driven channel. The CO^+, produced through the reaction of C^+ with OH, reacts with H_2 to form HCO^+, which dissociatively recombines to CO. This is the start of the C^+/C/CO transition zone. Neutralization of C^+ through charge transfer with atomic S becomes a dominant source of C. Eventually, PDR chemistry gives way to standard dark cloud, ion-molecule chemistry (Prasad & Huntress 1980, Herbst & Leung 1989). Formation of OH and H_2O is now initiated through the reaction of H_3^+ with O. Reactions of atomic O with OH then forms O_2.

2.3 *Cooling*

The gas in PDRs is cooled by FIR fine structure lines, such as [C II] 158 μm, [O I] 63, 146 μm, [Si II] 35 μm, [C I] 609, 370 μm, by H_2 rovibrational, and by molecular rotational lines, particularly of CO. For high densities and G_0, the gas at the surface of the PDR attains temperatures $\gtrsim$5000 K, and significant cooling in [Fe II] (1.26 and 1.64 μm), [O I] 6300 Å, and [S II] 6730 Å results (Burton et al 1990b). Convenient fitting formulae for the collisional excitation rates have been published by Tielens & Hollenbach (1985a), Hollenbach & McKee (1989), and Spaans et al (1994) for the atomic fine structure and forbidden lines, by Hollenbach & McKee (1979) and McKee et al (1982) for rotational transitions of CO, and by Martin & Mandy (1995) and Martin et al (1996) for rovibrational transitions of H_2. At high density, cooling by collisions with the cooler dust grains may be significant (Burke & Hollenbach 1983). The local radiative-cooling rate of a species is also affected by radiative transfer and, hence, depends on the global distribution of the level populations throughout the PDR. Generally, the escape-probability formalism is used to calculate the local cooling rate. As a result, in semi-infinite slabs the PDR temperature

structure can be calculated from the outside to the inside without the need for global iterations. However, for clumpy and turbulent clouds, more sophisticated techniques are required when photons escape through 4π steradians (sr) (Köster et al 1994, Störzer et al 1996) and when line transfer occurs between clumps or between clumps and interclump medium (Hegmann & Kegel 1996, Spaans 1996).

2.4 *Heating*

Two main mechanisms couple the gas to the FUV photon energy of stars: the photoelectric effect on PAHs and small dust grains and FUV pumping of H_2 molecules. Other heating mechanisms—gas collisions with warm grains, cosmic ray ionization and excitation, ionization of C, pumping of gas particles to excited states by the FIR radiation field of the warm dust followed by collisional deexcitation—play only a limited role in the heating or become important at great depth in the PDR (Tielens & Hollenbach 1985a).

PHOTOELECTRIC HEATING Photoelectric heating is dominated by the smallest grains present in the ISM (Watson 1972, Jura 1976). In recent years, it has become abundantly clear that large PAHs are an important component of the ISM (cf Allamandola et al 1989, Léger & Puget 1989), and these molecular-sized species may play an important role in the heating of interstellar gas (d'Hendecourt & Léger 1987, Lepp & Dalgarno 1988, Verstraete et al 1990, Bakes & Tielens 1994).

Figure 6 schematically shows the physics associated with the photoelectric effect on interstellar grains and PAHs. FUV photons absorbed by a grain create energetic (several electron volts) electrons. These electrons may diffuse in the grain, reach the surface, overcome the work function W of the grain and any Coulomb potential ϕ_c if the grain is positively charged, and be injected into the gas phase with excess kinetic energy. The efficiency ϵ_{grain} of the photoelectric effect on a grain, or the ratio of gas heating to the grain FUV absorption rate, is then given by the yield Y, which measures the probability that the electron escapes, times the fraction of the photon energy carried away as kinetic energy by the electron. For large grains and photon energies well above threshold, the photons are absorbed $\sim$100 Å inside the grain and the photoelectrons rarely escape ($Y \sim 0.1$) (Watson 1972, Draine 1978, Bakes & Tielens 1994).

Whereas some of the photon energy may remain behind as electronic excitation energy ($\sim$0.5), the yield is much higher for planar PAH molecules. The limiting factor is now that the ionization potential IP of a charged PAH can be larger than 13.6 eV, and absorbed FUV photons do not lead to the creation of a photoelectron. For example, the second ionization potential of pyrene, $C_{16}H_{10}$, is 16.6 eV, well above the hydrogen ionization limit (Leach 1987). The

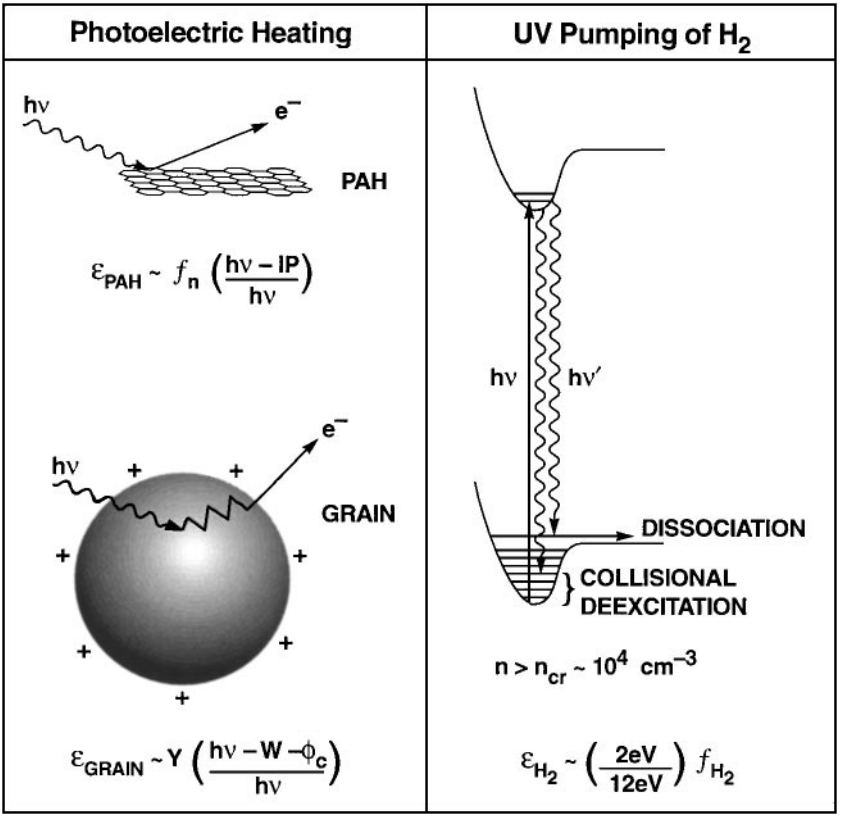

Figure 6 A schematic of the photoelectric heating mechanism (*left*). An FUV photon absorbed by a dust grain creates a photoelectron that diffuses through the grain until it loses all its excess energy in collisions with the matrix or finds the surface and escapes. For PAHs, the diffusion plays no role. A schematic of the H_2 heating mechanism for PDRs (*right*). FUV fluorescence can leave a H_2 molecule vibrationally excited in the ground electronic state. Collisional de-excitation of this excited molecule can then heat the gas. In about 10–15% of the pumping cases, the cascade goes to the vibrational continuum of the ground electronic state, which leads to photodissociation of the H_2 molecule. Simple expressions for the heating efficiencies, ϵ, of these different processes are indicated. See text for details.

photoelectric heating efficiency, ϵ_{PAH}, for small PAHs is then reduced by the fraction, f_n, of PAHs that can still be ionized by FUV photons.

Theoretical calculations show that PAHs and small (<50 Å) grains are more efficient heating agents of the gas than large grains. Interstellar grain size distributions are typically assumed to have number of grains per unit size interval

proportional to $a^{-3.5}$, where a is the grain radius (Mathis et al 1977, MRN). For an MRN distribution extending into the molecular PAH domain, about half the gas heating is due to grains with sizes less than 15 Å (Bakes & Tielens 1994). The other half originates in grains with sizes between 15 and 100 Å. Grains larger than 100 Å contribute negligibly to the photoelectric heating of the interstellar gas.

The photoelectric heating efficiency, ϵ, depends on the charge of a grain. A higher charge implies a higher Coulomb barrier (i.e. higher ionization potential) that has to be overcome. Thus, a smaller fraction of the electrons "dislodged" in the grain will escape. Moreover, those that do escape will carry away less kinetic energy (de Jong 1977). For PAHs, the charge determines whether further ionizations can still occur. Hence, the photoelectric heating efficiency will depend on the ratio, γ, of the photoionization rate over the recombination rate of electrons with grains/PAHs. When γ ($\propto G_0/n_e$) is small, grains/PAHs are predominantly neutral and the photoelectric heating has the highest efficiency ($\epsilon \sim 0.05$). When γ increases, the grains/PAHs become positively charged and the photoelectric efficiency drops. Based upon extensive theoretical calculations, simple analytical formulae for ϵ have been derived (Bakes & Tielens 1994).

H_2 HEATING As discussed in Section 2.2 the line absorption of an FUV photon will pump H_2 molecules to a bound excited electronic state, from which it will fluoresce back to the vibrational continuum of the ground electronic state and dissociate (10–15% of the time) or it will fluoresce back to an excited vibrational state in the electronic ground state (85–90% of the time; Figure 6). At low densities, the excited (bound) vibrational states can cascade down to the ground vibrational state through the emission of IR photons, giving rise to a characteristic far-red and near-IR rovibrational spectrum (see Section 4.2). At high densities, i.e. $n \gtrsim 10^4$ cm^{-3} (Martin & Mandy 1995, Martin et al 1996), collisions with atomic H can also be an important deexcitation mechanism, leading to heating of the gas and thermalization of the rovibrational states. The heating efficiency of this process is then approximately $\epsilon_{H_2} \simeq (E_{vib}/h\nu)\, f_{H_2} \simeq 0.17\, f_{H_2}$. The fraction of the FUV photon flux pumping H_2, f_{H_2}, depends on the location of the H/H_2 transition zone. Thus, when $G_0/n < 10^{-2}$ cm^3 (Section 2.2), H_2 self-shielding is important, the H_2 transition is near the surface, and most of the photons that can pump H_2 are absorbed by H_2 rather than dust. Under these conditions, $n > 10^4$ cm^{-3}, $G_0/n < 10^{-2}$ cm^3, $f_{H_2} \simeq 0.25$, and this heating process provides an efficient coupling to the FUV photon flux of the star. Sternberg & Dalgarno (1989) and Burton et al (1990b) describe how H_2 heating depends on G_0 and n.

3. PDR MODELS

3.1 *Steady-State Stationary PDR Models*

Considerable effort has been expended over the past two decades in constructing PDR models with the assumption of thermal and chemical balance and ignoring any flow through the PDR. Basically, this is equivalent to assuming that the time scale for H_2 formation on grains, $\tau_{H_2} \sim (10^9\ \mathrm{cm}^{-3}/n)$ years, which dominates the chemical time scales, is short compared to the dynamical time scales or the time scales for significant change in the FUV flux. Equilibrium PDR models of the transition of H to H_2 and C^+ to CO, including dust attenuation and self-shielding of the FUV flux, have a long history (Hollenbach et al 1971, Jura 1974, Glassgold & Langer 1975, Langer 1976, Clavel et al 1978, Federman et al 1979, deJong et al 1980, Viala 1986, Abgrall et al 1992, Heck et al 1992, Andersson & Wannier 1993, Draine & Bertoldi 1996). Models focusing on the H_2 spectrum are discussed in Section 4.2, and references to diffuse and translucent cloud models can be found in Section 2.2. However, intense FUV fields ($G_0 >> 1$) and high A_v often characterize dense PDRs. Tielens & Hollenbach (1985a), Sternberg & Dalgarno (1989), Hollenbach et al (1991), Abgrall et al (1992), LeBourlot et al (1993), and Diaz et al (1996) model the thermal balance and chemistry in homogeneous PDRs subjected to a range of elevated FUV fluxes.

Generally, these models consider a plane-parallel semi-infinite slab illuminated from one side by an intense FUV field (Figure 7). The penetrating FUV photons create an atomic surface layer. At a depth corresponding to $A_v \simeq 2$, the transition from atomic H to molecular H_2 occurs. Because of rapid photodestruction, vibrationally excited molecular hydrogen, H_2^*, does not peak until $A_v \sim 2$. Because of dust attenuation, the carbon balance shifts from C^+ to C and CO at $A_v \simeq 4$. The second peak in the neutral carbon abundance results from charge exchange between C^+ and S. Except for the oxygen locked up in CO, essentially all the oxygen is in atomic form until very deep in the cloud $A_v \sim 8$. Because of their low ionization potential, trace species such as S can remain ionized through a substantial portion of the PDR.

Besides the chemical composition, the FUV photons also control the energy balance of the gas through the photoelectric effect (cf Section 2.4). Typically, about 0.1–1% of the FUV energy is converted into gas heating this way. The rest is emitted as FIR dust continuum radiation. The gas in the surface layer is then much warmer ($\simeq$500 K) than the dust (30–75 K). Somewhat deeper into the PDR ($A_v > 4$), penetrating red and near-IR photons keep the dust warm and gas-grain collisions couple the gas temperature to slightly below the dust temperature. In PDRs, the gas cools through the FIR fine structure lines of mainly [O I] 63 μm and [C II] 158 μm at the surface and the rotational lines of CO deeper into the PDR. Figure 7 quantitatively shows this chemical and thermal structure.

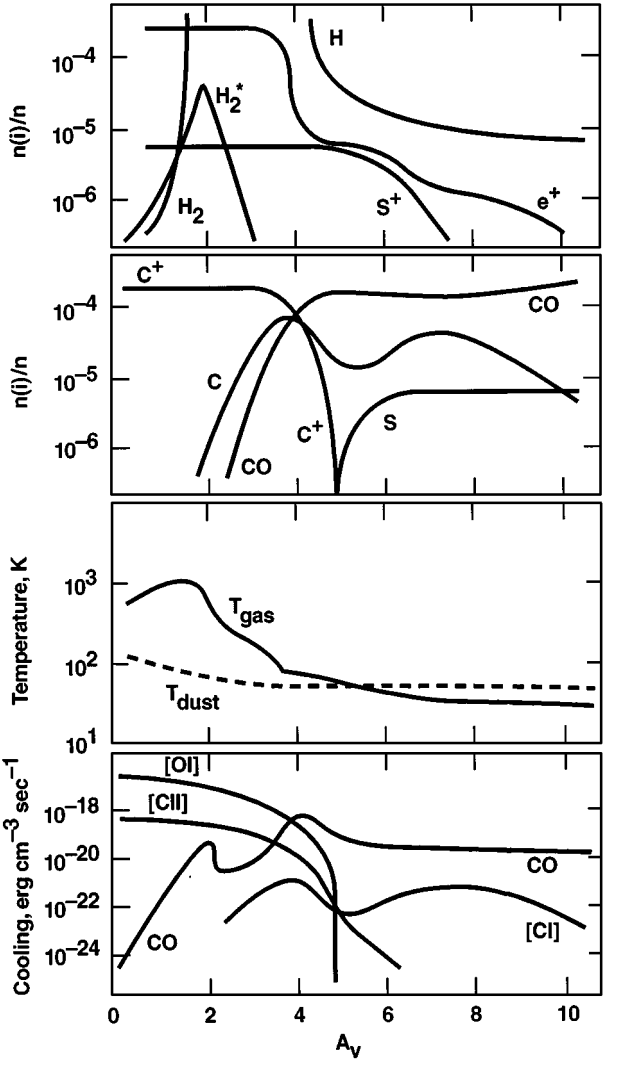

Figure 7 Calculated structure of the PDR in Orion ($n = 2.3 \times 10^5$ cm^{-3}, $G_0 = 10^5$) as a function of visual extinction, A_V, into the PDR (Tielens & Hollenbach 1985b). The illuminating source is to the left. *Top two panels*: Abundances relative to total hydrogen. *Third panel*: Gas and dust temperatures. *Bottom panel*: Cooling in the various gas lines.

Specialized aspects of PDR phenomena have been discussed in several papers: the origin of atomic carbon and [C I] 370, 609 μm emission (Tielens & Hollenbach 1985c, van Dishoeck & Black 1988, Flower et al 1994), PDRs around cooler sources such as F, A, and B stars or the central stars of protoplanetary nebulae (Roger & Dewdney 1992, Spaans et al 1994), the near-IR C I (9850 Å) emission (Escalante et al 1991), carbon radio recombination emission (Natta et al 1994), OH and CH_3OH abundances and masers (Hartquist & Sternberg 1991, Hartquist et al 1995), CO^+ abundances (Latter et al 1993, Störzer et al 1995), and molecular chemistry in general (Fuente et al 1993, Sternberg & Dalgarno 1995). Recently, models have been constructed of clumpy PDRs, many of them focused on the C^+/C/CO transition and the origin of [C I], H_2 2 μm, and CO rotational emission (Burton et al 1990b, Tauber & Goldsmith 1990, Gierens et al 1992, Meixner & Tielens 1993, Wolfire et al 1993, Köster et al 1994, Hegmann & Kegel 1996, Spaans 1996, Störzer et al 1996).

3.2 *Time-Dependent and Nonstationary PDRs*

There are two basic phenomena that can cause significant time-dependent effects on the chemical abundances and temperatures in a PDR. The first is when G_0 or n changes in a smaller time scale than τ_{H_2}. For example, an O or B star suddenly "turns on" in a cloud, clumps moving in PDRs produce rapid shadowing effects, or a PDR shell quickly expands around the central star of a planetary nebula. The second is when, in the frame of the ionization front, the neutral gas flows through the PDR (hence "nonstationary PDR") in a time that is short compared to τ_{H_2}. In this case, the chemical and thermal structure can achieve a steady state, but the resulting structure differs from the structure of a stationary PDR because of the rapid advection of molecular material from the shielded regions into the surface zones.

Hill & Hollenbach (1978), London (1978), and Roger & Dewdney (1992) have considered the time-dependent evolution of the ionization front and H_2 dissociation front when O or B stars suddenly turn on in a neutral cloud. Goldshmidt & Sternberg (1995) looked in detail at the enhancement of H_2 fluorescent emission when a low ($n \lesssim 10^4$ cm^{-3}) constant-density molecular cloud is suddenly illuminated with intense FUV; Hollenbach & Natta (1995) examined the collisionally modified H_2 spectra when $n > 10^4$ cm^{-3}. Störzer et al (1997) studied the temporary enhancement of C^0 abundance and [C I] emission caused by C^+ recombination when the FUV flux is suddenly shadowed by moving opaque clumps. Monteiro (1991) found a similar enhancement for rotating clumps in PDRs. Gerola & Glassgold (1978), Tarafdar et al (1985), Prasad et al (1991), Heck et al (1992), Lee et al (1996), and Nelson & Langer (1997) examined the time-dependent evolution of diffuse atomic clouds into

molecular clouds. Lee et al (1996) also studied the time-dependent chemistry of an inhomogeneous molecular cloud suddenly exposed to FUV radiation.

The first PDR modeling that incorporated fast flows or advection were chemical models that used rapid turbulent eddies or diffusion to mix molecular gas from opaque molecular cores with surface photodissociated gas (Phillips & Huggins 1981, Boland & deJong 1982, Chieze & Pineau des Forêts 1989,1990, Chieze et al 1991, Williams & Hartquist 1984, 1991, Xie et al 1996). Recently, Bertoldi & Draine (1996) have discussed in detail the time-dependent effect on the PDR structure of the advance of the ionization front (IF) and dissociation front through a cloud. In this case the "flow" velocity is equivalent to the speed of the IF advancing into the PDR. The advected flow is relatively fast when the photoevaporating H II gas is free to flow to lower pressure regions, such as when neutral clumps photoevaporate well inside an H II region. Assuming approximately thermal pressure equilibrium between the photoevaporating H II gas and the neutral PDR gas on the other side of the IF, and assuming a typical PDR temperature of $\sim$1000 K, the PDR density $n_{PDR} \simeq 20 n_{HII}$. Assuming the free-flowing H II gas evaporates from the IF at a speed comparable to its thermal speed, i.e. $c_{HII} \sim 10$ km s^{-1}, the flow speed $v_{PDR} \sim (n_{HII}/n_{PDR}) c_{HII}$ through the PDR is about 0.5 km s^{-1}. The flow time through the PDR is as follows: $\tau_{PDR} \simeq (N_{PDR}/n_{PDR})/v_{PDR}$. Equating τ_{PDR} to τ_{H_2}, we obtain a critical flow speed of $\sim$0.7 km s^{-1}, above which the H_2 abundance may be significantly higher than its "stationary" (no-flow) value.

The fact that for free-flowing gas the estimated v_{PDR} is so close to the estimated critical speed indicates that nonstationary PDRs may be important. Bertoldi & Draine (1996) show how v_{PDR} can be related to the EUV flux reaching the IF, because these photons create the new ionizations that push the IF into the PDR. The EUV flux depends on the gas and dust attenuation in the ionized gas and the morphology (e.g. size of clump and distance from star) of the region. This morphology determines the geometric dilution of the flux and the EUV attenuation by recombined atomic hydrogen in the predominantly ionized, evaporative flow. They conclude that for a broad range of conditions, including the famous PDR in Orion (Figures 1 and 2), time-dependent effects may be of some importance.

Much larger effects can be expected when the H_2 survives all the way to the IF as it flows from the opaque regions, leading to the merging of the dissociation front (DF) with the IF. Bertoldi & Draine (1996) have quantitatively determined when the IF merges with the DF. Qualitatively, the merger tends to occur for hotter stars (with a high ratio of EUV photons to FUV photons) illuminating clumps or clouds with a geometry such that relatively little attenuation of the EUV flux occurs by recombining hydrogen in the evaporating flow or H II region (e.g. a small, freely evaporating clump near the hot star). Apparently,

the condition is not met in the Orion Bar (Figure 2) because the observed layered structure clearly shows the H_2 offset from the IF; in fact, Tielens et al (1993) and van der Werf et al (1996) find good agreement with steady-state stationary PDR models.

The consequences of rapid advection through PDRs have not yet been fully determined. Bertoldi & Draine (1996) suggest that H_3^+ may be produced in a merged IF/DF and that enhanced H_2 IR emission and reduced H I columns will result. Nonstationary PDR models may find interesting application in the photoevaporating protoplanetary disks (proplyds) found in the Orion nebula (Churchwell et al 1987, O'Dell et al 1993).

4. OBSERVATIONS OF DENSE PDRs IN THE GALAXY

Dense PDRs are bright in the FIR dust continuum, the PAH emission features, the FIR fine structure lines of [O I] and [C II], and the rotational lines of CO. Besides these dominant cooling processes, PDRs are also the source of (fluorescent or collisionally excited) rovibrational transitions of H_2 in the near IR; the atomic fine structure lines of [C I] 609, 370 μm, and [Si II] 35 μm; and the recombination lines of C I in the radio (e.g. C91α) and the far red (e.g. 9850 and 8727 Å). They are also observed in rotational transitions of trace molecules like CO^+, CN, and C_2H.

4.1 *Physical Conditions*

These observations can be used to determine the physical conditions in the emitting gas. The FIR fine structure lines are particularly useful in that respect because the critical densities of the [C II] and [O I] lines (3×10^3–3×10^5 cm^{-3}) and excitation energies (100–300 K) span the n,T range present in many dense PDRs. The [C II] 158 μm line, which is (marginally) optically thin, can be used to determine the total mass of emitting gas. These analyses do require assumed elemental abundances (or abundance ratios) for those species that are somewhat uncertain (cf Cardelli et al 1996, Mathis 1997). Often, the physical conditions (e.g. densities) are also constrained by the ratio of the total cooling rate (i.e. the [O I] + [C II] intensity) to the FIR dust continuum. This ratio is approximately equal to the photoelectric heating efficiency, which depends on the local density through the charging of the grains (cf Section 2.4). Of course, this analysis requires a good understanding of the photoelectric heating process itself and hence is also uncertain. Boreiko & Betz (1996a,b) have derived temperatures, column densities, and $^{12}C/^{13}C$ isotopic ratio ($\simeq$58) in M42 by observing the [O I] 63 μm and both isotopic [C II] 158 μm lines with very high velocity resolution. The derived temperatures ($\sim$200 K) are somewhat lower and columns ($\sim 10^{22}$ cm^{-2}) somewhat higher than homogeneous PDR models.

The temperature and column density can also be determined directly from the lowest pure rotational lines of H_2, which have very low critical densities. To date, that has only been done for the Orion Bar (Parmar et al 1991, Burton et al 1992b) and S140 (Timmermann et al 1996). The intensity distribution of the rotational CO levels also provides density and temperature information, albeit for the molecular component in the PDR ($A_v \simeq 4$) (Harris et al 1985, Jaffe et al 1990, Stutzki et al 1990, Graf et al 1993, Howe et al 1993, Lis et al 1997). Generally, the J = 7–6 transition is quite strong in PDRs, implying densities of $\sim 10^5$ cm^{-3} and temperatures of $\sim$150 K. The presence of CO J = 14–13 emission in some sources (Stacey et al 1993) indicates even higher densities and temperatures (10^7 cm^{-3}; 500 K).

In Figure 8, observations of the [C II] 158 μm and [O I] 63 μm lines are plotted as a function of the intensity of the incident FUV field, G_0 ($= I_{IR}/2.6 \times 10^{-4}$ erg cm^{-2} s^{-1} sr^{-1}, where I_{IR} is the observed IR intensity). Examining these observations, we conclude that the [C II] line dominates the cooling for $G_0 \lesssim 10^3$. The [O I] line dominates at higher G_0. Typically, the total cooling line intensity is in the range 10^{-2}–10^{-3} of the total FIR continuum intensity, in agreement with predicted grain photoelectric heating efficiencies of 10^{-2}–10^{-3} (see Section 2.4). This rough correlation extends over a large range in G_0 and an even larger range in luminosity (10^4–10^{11} L$_\odot$) (Hollenbach 1990).

Also shown in Figure 8 are PDR model calculations for different densities (Hollenbach et al 1991). In the models, the [C II] intensity scales with the incident FUV flux (or FIR intensity) at low G_0 where [C II] is the dominant cooling line. The [C II] intensity levels off at high G_0 when the temperature exceeds $\sim$100 K. At that point, [O I] 63 μm becomes a better coolant and its intensity scales with G_0. The models are in good agreement with the observations for densities in the range 10^3–10^5 cm^{-3}. We note that, as expected, the PDRs in reflection nebulae, such as NGC 7023, and bright rim clouds, such as S140, are characterized by somewhat lower densities (3×10^3 cm^{-3}) and incident FUV fields than those surrounding H II regions, such as M42 in Orion (10^5 cm^{-3}).

We summarize the physical conditions in PDRs associated with a number of template objects as derived from observations in Table 1. Typical densities and temperatures are $n \sim 10^3$–10^5 cm^{-3} and $T \sim$ 200–1000 K. The atomic mass in the C^+ zone, M_a, is a significant fraction of the molecular cloud (core) mass, M_m (see also Tielens 1994).

In general, observations reveal pronounced clumping of the emitting gas. First, the [O I], [C II], and [C I] emission is extended on $\gtrsim 5'$ scale, as illustrated in Figure 1 for Orion A. In fact, Stacey et al (1993) trace the [C II] extent even further than Figure 1, and likewise PDR H_2 emission has been observed in Orion A on larger scales by Burton & Puxley (1990), Luhman et al (1994), and Usuda et al (1996). All this gas is photoionized, photodissociated, and

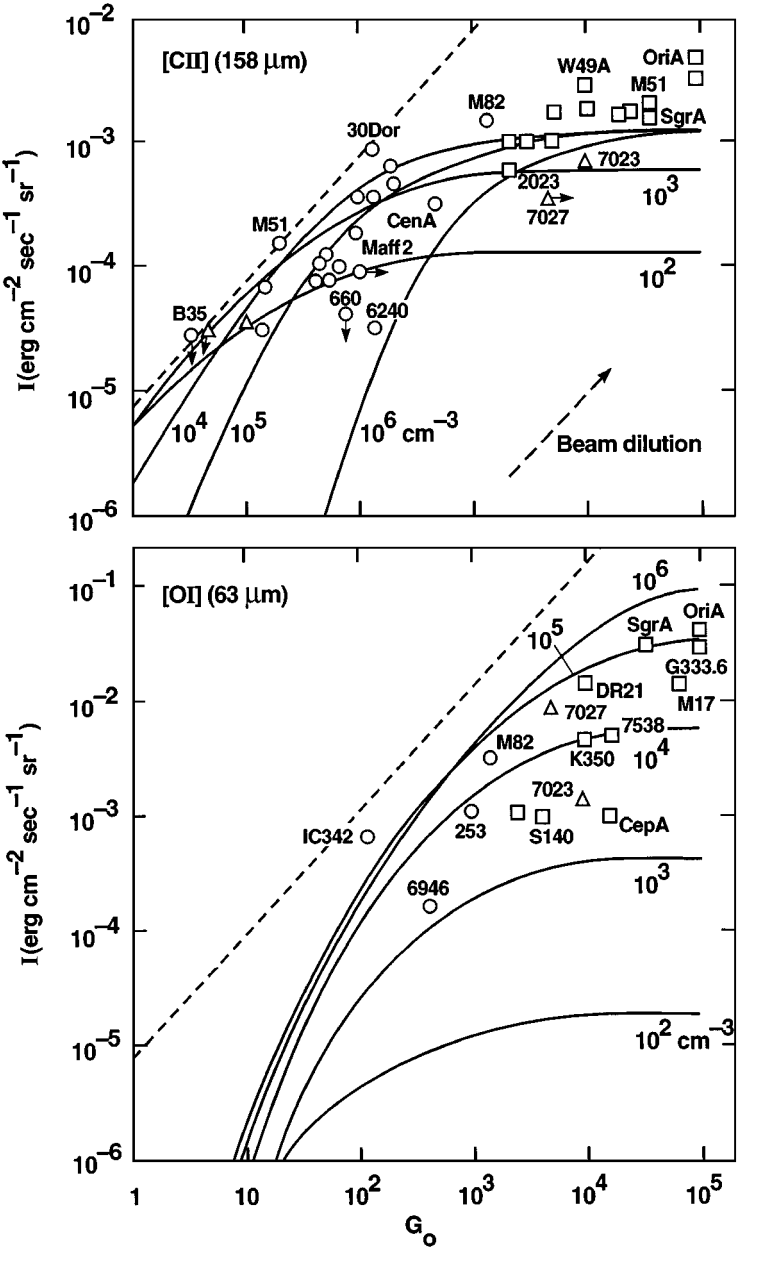

(photo)heated by θ^1C Ori. Similar results have been obtained for Orion B, M17, S140, NGC 2023, and many other sources (Stutzki et al 1988, Matsuhara et al 1989, Howe et al 1991, White & Padman 1991, Stacey et al 1993, Jaffe et al 1994, Plume et al 1994, Herrmann et al 1997, Luhman & Jaffe 1996, Spaans & van Dishoeck 1997). This emission scale size is much larger than expected for a homogeneous region at the density indicated by the line ratios. Clearly, the gas is organized in filamentary and clumpy structures that allow the penetration of FUV photons to very large distances from the illuminating stars. Second, maps in many molecular species (i.e. ^{13}CO, C^{18}O, CS, NH_3, HCO^+, HCN, H_2, and PAHs) show direct evidence for clumping in PDRs with a surface filling factor of $\simeq$0.1 (Gatley et al 1987, Güsten & Fiebig 1988, Massi et al 1988, Stutzki et al 1988, Stutzki & Güsten 1990, Tauber & Goldsmith 1990, Chrysostomou et al 1992, 1993, Minchin et al 1993, Hobson et al 1994, Tauber et al 1994, Kramer et al 1996, Lemaire et al 1996; R Young Owl, M Meixner, M Wolfire & AGGM Tielens, in preparation). Third, most PDRs show bright molecular lines [e.g. CO J = 14–13, H_2 1–0 and 2–1 S(1)] with high critical densities and high excitation temperatures that attest to the presence of high-density warm molecular gas. The physical conditions of these clumps are not well constrained and likely span a range of values. Thermal H_2 2–1 S(1)/1–0 S(1) ratios require densities $n \gtrsim 10^5$ cm^{-3} and $T \sim 1000$ K. Likewise, C II recombination line studies indicate clumpy high-density ($\sim 10^5$–10^6 cm^{-3}) regions over a large area of the PDRs in Orion and NGC 2023 (Natta et al 1994, Wyrowski et al 1997). Somewhat higher densities, $n \gtrsim 10^6$–10^7 cm^{-3} are required to produce bright CO J = 14–13, 17–16, or 23–22 emission. Table 1 lists estimates for clump physical conditions in several PDRs. We note that homogeneous PDR models fall typically short of observed mid-J (e.g. 6–5 or 7–6) CO intensities, especially from the ^{13}CO isotope (Graf et al 1993, Lis et al 1997). Clump models may resolve this discrepancy (Köster et al 1994), or it may be that models underestimate the gas temperatures in the C^+/C/CO transition regions where these lines originate (Tauber et al 1994).

The inferred thermal pressures for these clumps (10^9–10^{10} K cm^{-3}) are well in excess of that sustainable by the interclump medium (or the H II region

←

Figure 8 Comparison of observations and models of the [C II] 158 μm and the [O I] 63 μm line are shown as a function of G_0 (Hollenbach et al 1991). Squares are PDRs associated with H II regions; triangles are PDRs associated with dark clouds, reflection nebulae, and planetary nebulae; and circles are PDRs associated with the inner 45–60″ of galaxies. Some well-known individual regions have been identified by their catalog numbers. The effects of beam dilution are indicated by the *dashed arrow*. The different models are labeled by their densities. The *dashed line* indicates an efficiency of 5% in the conversion of FUV photons energy into gas cooling—the maximum expected for the photoelectric effect. See text for details.

Table 1 Characteristics of PDRs

Object	NGC 2023	Orion Bar	NGC 7027	Sgr A	M 82
Line intensities[a]					
[OI] 63 μm	4. (−3)	4. (−2)	1. (−1)	2. (−2)	1. (−2)
[OI] 145 μm	2. (−4)	2. (−3)	5. (−3)	7. (−4)	1.5 (−4)
[SiII] 35 μm	2. (−4)	9. (−3)	—	2. (−2)	1. (−2)
[CII] 158 μm	7. (−4)	6. (−3)	1. (−2)	2. (−3)	2. (−3)
[CI] 609 μm	—	5. (−6)	1.8 (−6)	4. (−5)	2. (−5)
H_2 1–0 S(1)	5. (−5)	2. (−4)	8. (−4)	9. (−4)	5. (−5)
CO J = 1–0	3. (−8)	4. (−7)	1.5 (−6)	7 (−7)	2.6 (−7)
CO J = 7–6	5. (−5)	2. (−4)	—[b]	1.5 (−3)	5. (−5)
CO J = 14–13	—	3. (−4)	—[b]	3. (−4)	—
FIR[c]	8. (−1)	5. (0)	4. (1)	5. (1)	6. (0)
PAHs[d]	9. (−2)	1.5 (−1)	1.8 (0)	—	1.4 (−1)
G_0	1.5 (4)	4. (4)	6. (5)	1. (5)	1. (3)
Physical conditions					
Interclump					
n [cm^{-3}]	7.5 (2)	5. (4)	1. (5)[e]	1. (5)	1. (4)
T [K]	250	500	1000[e]	500	250
M_a/M_m	0.2	0.6	0.3	0.04	0.1
Clump					
n [cm^{-3}]	1. (5)	1. (7)	1. (7)[e]	1. (7)	—
T [K]	750[f]	(2000)	(2000)[e]	(2000)	—
f_v	0.1	0.005	0.05	0.06	4. (−4)
References[g]	1–5	6–8	9–13	13–16	14, 17–19

[a]Intensities in units of erg cm^{-2} s^{-1} sr^{-1}.

[b] Bright CO J = 17–16 has been observed by Justtanont et al (1997).

[c]Total far IR dust continuum intensity.

[d]Intensity in the PAH emission features.

[e]Interclump and clump refer to halo and torus, respectively (Justtanont et al 1997).

[f]C91α indicates 100–200 K (Wyrowski et al 1997).

[g]References: 1, Steiman-Cameron et al (1997); 2, Wyrowski et al (1997); 3, Sellgren et al (1985); 4, Jaffe et al (1990); 5, Gatley et al (1987); 6, Tielens et al (1993); 7, Tauber et al (1994; 1995); 8, Stutzki et al (1990); 9, Cohen et al (1985); 10, Justtanont et al (1997); 11, Keene (1995); 12, Graham et al (1993); 13, Burton et al (1990a); 14, Wolfire et al (1990); 15, Harris et al (1985); 16, Serabyn et al (1994); 17, Willner et al (1977); 18, Genzel (1992); 19, Schilke et al (1993).

pressure). These clumps may therefore be confined by self-gravity and either are on their way to forming stars or already contain an embedded protostar (Meixner et al 1992). Hence, they may be the PDR counterparts of the small partially ionized (Bok) globules (PIGs) and stellar proplyds observed in H II regions (Churchwell et al 1987, O'Dell et al 1993). These objects seem to be widespread in the molecular clouds.

4.2 *The H_2 Spectrum*

FUV absorption in the Lyman Werner bands excites molecular hydrogen electronically. Electronic (FUV) fluorescence (Sternberg 1989) leaves the molecule in a vibrationally excited state of the ground electronic state 85–90% of the time (Section 2.4, Figure 6). Molecules in these levels decay through electric quadrupole transitions in the far red and near IR. The intensities of these lines depend then on the detailed distribution of the level populations through the cloud, which themselves depend on the (FUV) line radiative transfer as well as the density and temperature of collision partners. Level populations and IR emission spectra have been calculated for a variety of model clouds by Black & Dalgarno (1976), Black & van Dishoeck (1987), Sternberg [1988, 1990 (for HD, i.e. hydrogen molecule where one of the hydrogens is deuterium)], Sternberg & Dalgarno (1989), Draine & Bertoldi (1996), and Neufeld & Spaans (1996). Pure rotational spectra of H_2 have been calculated by Burton et al (1992b) and by Spaans et al (1994).

At low n ($\lesssim 10^4$ cm^{-3}), collisional de-excitation is unimportant and the IR spectrum is due to "pure" fluorescence and can be calculated directly from the transition probabilities of the levels involved, taking the radiative transfer into account. For $G_0/n < 10^{-2}$ cm^3, H_2 self-shielding dominates the opacity in the 912–1100 Å range and the line intensity scales directly with the intensity of the incident FUV radiation field. For $G_0/n \gtrsim 0.1$ cm^3, dust opacity is more important and the line intensities become largely independent of G_0. At high densities, collisional processes are important, modifying the emitted spectrum to a thermal spectrum in the lowest levels (i.e. v = 1–0 and 2–1) (Sternberg & Dalgarno 1989, Burton et al 1990b, Draine & Bertoldi 1996, Luhman et al 1997). The population of high vibrational (v) levels, though reduced by collisions, is caused by FUV pumping.

Far-red and near-IR H_2 fluorescence spectra have been observed in a variety of classical PDRs such as those associated with NGC 2023, S140, NGC 7023, the Orion Bar, Orion A and B, and ρ Oph (Hayashi et al 1985, Gatley et al 1987, Hasegawa et al 1987, Hippelein & Münch 1989, Tanaka et al 1989, Burton et al 1990a, 1992a, Luhman & Jaffe 1996). Figure 9 compares the observed IR spectrum 160″ north of the illuminating star in NGC 2023 (Gatley et al 1987) with model calculations for the pure fluorescence case, illustrating the good fit possible (Black & van Dishoeck 1987). The fit mainly depends on the adopted value for G_0 and the detailed geometry of this emission ridge. It is not sensitive to the density for $n \lesssim 10^4$ cm^{-3}. The more thermal 1–0 S(1)/2–1 S(1) ratio observed for the bright H_2 ridge, 78″ south of the star indicates emission by higher density gas (10^5 cm^{-3}; Burton et al 1992a, Draine & Bertoldi 1996), in good agreement with studies of the dominant PDR cooling lines and molecular

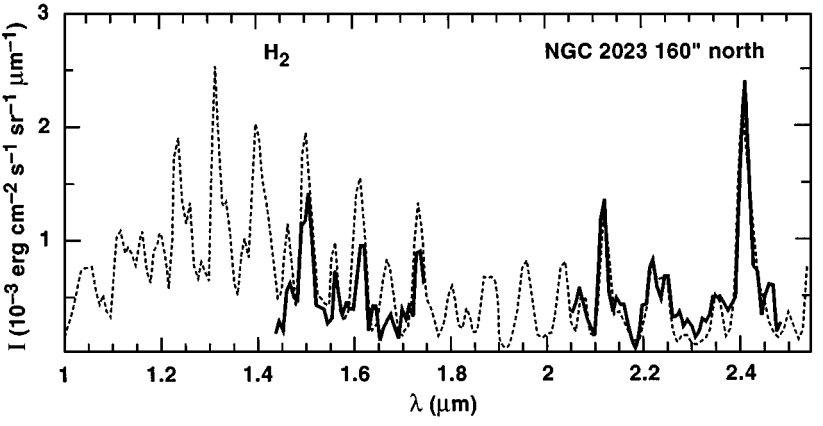

Figure 9 Comparison of observed and calculated H_2 emission spectra, adapted from Black & van Dishoeck (1987). *Solid curve*: spectrum observed 160″ north of the illuminating star in the reflection nebula, NGC 2023 (Gatley et al 1987). *Light curve*: Calculated emission spectrum for $G_0 \simeq 200$ and a density of 10^4 cm^{-3} convolved to a resolution of $\lambda/\Delta\lambda \simeq 100$ (Black & van Dishoeck 1987). See text for details.

line observations (Steiman-Cameron et al 1997, Jansen et al 1995a, Fuente et al 1995, Wyrowski et al 1997).

4.3 *The Molecular Transition Observed in Edge-On PDRs*

The edge-on geometry of the Orion Bar PDR lends itself particularly well to detailed studies of the spatial structure of PDRs (cf Tielens et al 1993, Hogerheijde et al 1995, van der Werf et al 1996; Figure 2). Clearly, the H/H_2 transition, as outlined by the emission from vibrationally excited H_2, occurs at about 10″ into the cloud from the ionization front (i.e. the location of the Bar in [O I] 6300 and [S II] 6731 Å). The CO 1–0 and [C I] 609 μm lines peak rather abruptly at a distance of 20″ of the ionization front. These observations agree very well with predictions of the global characteristics of stationary PDR models (Tielens et al 1993, Jansen et al 1995a, van der Werf et al 1996). In such models, the location of the H/H_2 transition region and the peak in H_2^* emission is displaced inwards from the ionization front by $A_v \simeq 2$, and the C^+/C/CO transition occurs another $\Delta A_v \simeq 2$ deeper into the cloud (Figure 7). Using standard dust parameters, the observed spatial scale translates then into a density of 5×10^4 cm^{-3} (Tielens et al 1993). Calculated line emission for the fine structure lines of [O I] 63 and 146 μm, [C II] 158 μm, [Si II] 35 μm, [C I] 609 μm, and CO 1–0 agree well with the observed intensities for this density and $G_0 = 5 \times 10^4$, which is appropriate for θ^1 C Ori at the projected distance of the Orion Bar (Table 1).

The presence of denser clumps (10^7 cm^{-3}) is indicated by bright emission in CO 7–6 and 14–13 (Stacey et al 1993).

M17-SW is another region where the edge-on geometry allows a detailed study of the structure of PDRs (Stutzki et al 1988, Meixner et al 1992). As in the Orion Bar region, cross scans show a clear separation between the ionized (free-free), atomic ([O I], [C II], [Si II]), and molecular (CO 2–1) gas. M17 is four times farther away than Orion, and the scale size is somewhat larger (40″ rather than 20″); both these factors indicate a much lower average gas density (3×10^3 cm^{-3}) in the interclump regions of this molecular cloud core. The observed high intensity of the [O I] and [Si II] lines implies then that they mainly originate from the surfaces of the dense ($n \lesssim 10^7$ cm^{-3}) clumps evident in the molecular observations (Stutzki et al 1988, Meixner et al 1992). The [C II] and [C I] lines in contrast originate from the lower density interclump gas in the M17-SW core. Besides the M17-SW PDR, the [C II] and [C I] emission extends over a size scale of $\simeq$10 pc (Stutzki et al 1988, Matsuhara et al 1989, Keene et al 1985). This emission may well be associated with clumps illuminated at large distances by FUV penetration through even lower density gas (see Section 4.4).

Edge-on PDRs form an excellent laboratory to study in detail the interaction of FUV photons with gas and dust. One might hope that future studies of, for example, the dominant gas cooling lines and their correlation with the PAH and dust IR emission will allow a semi-empirical evaluation of the cooling and, hence, photoelectric heating process and its dependence on physical conditions. Present and future generations of (sub)millimeter arrays also allow a detailed analysis of the effects of FUV photons on the molecular composition of interstellar gas. The first studies of this kind have already been undertaken for IC 63 (Jansen et al 1995b, 1996), the Orion Bar (Tauber et al 1994, 1995, Hogerheijde et al 1995, van der Werf et al 1996, Fuente et al 1996; R Young Owl, M Meixner, M Wolfire & AGGM Tielens, in preparation), and NGC 2023 (Fuente et al 1995). Finally, limb brightening due to the edge-on geometry also allows the detection of trace species that are otherwise difficult to detect, for example, CO^+ (Latter et al 1993, Jansen et al 1995a, Störzer et al 1995).

4.4 *The Origin of [C I] Emission*

In retrospect, observations of the [C I] 609 μm line formed one of the earliest indications that PDRs are a ubiquitous component of molecular clouds (Phillips & Huggins 1981). Atomic carbon has long been recognized to be an abundant species near the surfaces of molecular clouds (Langer 1976, de Jong et al 1980). However, the early observations of the lowest lying transition of [C I] showed more intense emission than expected on the basis of the predicted C I column density. While this discrepancy led to a flurry of papers proposing a variety of

schemes to increase the abundance of atomic carbon inside dense clouds, the first detailed PDR models (Tielens & Hollenbach 1985a–c) calculated about a 10-times higher C I column density than the earlier models, partly due to improved chemical schemes (i.e. charge exchange between C^+ and S and self-shielding of C I) and partly because of an adopted higher gas-phase carbon abundance. PDR theory (Tielens & Hollenbach 1985a,c, van Dishoeck & Black 1988, Hollenbach et al 1991) is now in reasonable agreement with the observed line intensities (Phillips & Huggins 1981, Keene et al 1985, Genzel et al 1988). Current models explore the effects of the clumpy structure of molecular clouds (Hegmann & Kegel 1996, Spaans & van Dishoeck 1997), the time-dependent effects associated with shadowing by moving clumps (Störzer et al 1997), and the dependence of C I on ionization (Flower et al 1994).

Higher spatial resolution studies with the James Clerke Maxwell Telescope and the Caltech Submillimeter Observatory clearly confirm the association of the [C I] emission with the PDR. In particular, in the Orion Bar, the [C I] 609 and 370 μm emission forms a bar-like structure at a similar distance from the ionization front as the CO 1–0, in good agreement with theory (White & Padman 1991, White & Sandell 1995, Tauber et al 1995). A similar spatial structure is seen in S140, although an embedded source contributes to the [C I] deeper into the cloud as well (Minchin et al 1993). Similar to the extremely extended [C II] 158 μm emission, the extended [C I] emission in M17 is thought to originate from the surfaces of clumps illuminated either by deeply penetrating FUV photons or by local B stars (Stutzki et al 1988, Meixner & Tielens 1993, Plume et al 1994). [C I] often correlates with ^{13}CO 2–1 in spatial extent and line profile (Keene et al 1997), indicating that emission of both species is dominated by clump PDR surfaces (Meixner & Tielens 1993, Spaans & van Dishoeck 1997).

4.5 *The [C II]–CO Correlation*

Crawford et al (1985) and Stacey et al (1991) show a linear correlation in the integrated intensities of [C II] 158 μm and ^{12}CO J = 1–0 in the observations of bright dense galactic PDRs and PDRs in starburst galactic nuclei. Wolfire et al (1989) explain this correlation with high FUV-field PDR models in which the [C II] 158 μm emission arises from the warm, $A_v \lesssim 1$–2, outer regions and the ^{12}CO J = 1–0 originates from the cooler gas somewhat deeper ($A_v \sim 3-4$) in the cloud. However, in low FUV fields, the [C II]/CO ratio is low because the PDR cools and self-shields, which affects [C II] much more than CO. On the other hand, high [C II]/CO ratios are found in CO-deficient (low A_v) regions such as diffuse clouds or H I halos of molecular clouds (Jaffe et al 1994). High ratios may also result from geometry effects (Köster et al 1994) or clouds with small molecular cores and large C^+ halos such as in the Magellanic Clouds

(Boreiko & Betz 1991, Rubio et al 1993a,b, Mochizuki et al 1994, Poglitsch et al 1995, Israel et al 1996). These trends are noted by Stacey et al (1991).

4.6 *Planetary Nebulae (PNe)*

Observations of H I, Na I, H_2, CO, and other trace molecules demonstrate that a significant mass of neutral PDR material, on the order of 1 $M_\odot$ compared to $\sim$0.1 $M_\odot$ of ionized gas, is associated with PNe (for references, see recent reviews by Huggins 1992, 1993, Dinerstein 1991, 1995, Tielens 1993). Clearly, studies of these PDRs are crucial for a proper understanding of the dynamic and morphologic evolution of the ejected material. Spherical shells tend to completely ionize in a relatively short time, $t \lesssim 10^3$ year (e.g. Bobrowsky & Zipoy 1989, Tielens 1993, Gussie et al 1995). However, observations of the ionized and neutral gas (e.g. Huggins et al 1992, Graham et al 1993, Latter et al 1995, Kastner et al 1996) clearly show that the ejecta is clumped or nonspherical (e.g. disk-like or torus-like), and PDR models confirm that in evolved ($t \gtrsim 10^3$ year) PNe, atoms and molecules will survive in dense ($n \gtrsim 10^5$ cm^{-3}) clumps even though the FUV fluxes are large ($G_0 \sim 10^4$–10^6) (Tielens 1993; A Natta & DJ Hollenbach, in preparation). Proper models require a time-dependent calculation of the partial shells or clumps, including the effects of rapid changes in the stellar effective temperature, G_0, and n, as well as the advance or retreat of the IF with respect to the PDR gas. The H_2 emission is often thermal emission of H_2 warmed in the PDR to $T \sim$ 1000–2000 K by grain photoelectric heating, H_2 FUV pump heating, and soft X-ray heating. Goldshmidt & Sternberg (1995) suggest that strong H_2 emission from young planetary nebulae is due to the H_2 enhancement caused by time-dependent PDR H_2 chemistry. Shock heating, often invoked in the past, may be less important than previously believed. Considerable work is underway to predict H I, [C II], [O I], H_2, and other molecular emission lines and to compare existing observations with the models to determine physical conditions such as the ejected mass (A Natta & DJ Hollenbach, in preparation; WB Latter, AGGM Tielens & DJ Hollenbach, in preparation).

4.7 *The Galactic Center*

The center of the Galaxy has been recently reviewed by Morris & Serabyn (1996) and Genzel et al (1994). PDR studies have delineated the structure, dynamics, and excitation mechanisms in the central $\sim$30 pc of the Galaxy. Lugten et al (1986), Genzel et al (1990), and Poglitsch et al (1991) show that a large fraction of the neutral gas, up to 10%, lies in C^+ regions, which suggests that most of the neutral gas is in PDRs. The large [C II] intensities from some clouds indicate that they are relatively close (<15 pc) to the galactic center, and connecting bridges suggest that the outlying clouds feed material into the center.

A prominent structure in the central 10 pc is the circumnuclear disk (CND) or torus, first observed in FIR continuum by Becklin et al (1982). Subsequent studies in [O I] (Genzel et al 1984, 1985, Jackson et al 1993), [C II] (Genzel et al 1985, Lugten et al 1986, Poglitsch et al 1991), [C I] (Serabyn et al 1994), [Si II] (Herter et al 1986, 1989, Graf et al 1988), and mid–J CO (e.g. Genzel et al 1985, Harris et al 1985) indicate a mass of 10^4–10^5 $M_\odot$, with an inner radius of about 1.5 pc and an outer radius $\gtrsim$8 pc. The atomic carbon is comparable to the CO abundance; this is 10 times its value in local GMCs. The CND seems to consist of several streamers of material and is quite clumpy and turbulent (Jackson et al 1993). Wolfire et al (1990) and Burton et al (1990b) compare PDR models to observations to derive an incident FUV flux $G_0 \sim 10^5$ from the central cavity, which illuminates a clumpy structure with densities ranging from 10^5–10^7 cm^{-3} (Table 1). Overall, there is evidence for a mass infall rate into the central $r < 1.5$-pc cavity of $\sim 10^{-2}$ $M_\odot$ year^{-1}, which can feed a central black hole or a future starburst (Jackson et al 1993). The existence of hot massive stars in the central cavity suggests a recent episode of star formation. At least 200 $M_\odot$ of neutral PDR gas has been observed in [O I] in the central cavity (Jackson et al 1993); this gas provides evidence for a possible building reservoir of material available for star formation.

5. APPLICATIONS OF PDR MODELS

5.1 *CO Line Profiles and the H_2 Mass to CO J = 1–0 Luminosity Ratio*

Because the optically thick ^{12}CO J = 1–0 emission originates largely from FUV heated PDRs on the "surfaces" of opaque molecular clouds, PDR modeling should be able to reproduce the CO line intensities and profiles. Tauber & Goldsmith (1990) and Wolfire et al (1993) construct models that self-consistently calculate the chemistry, thermal balance, and radiative transfer appropriate for a PDR model. They conclude that clumpy models can reproduce the observed centrally peaked profiles; Falgarone et al (1994) point out that turbulent velocity fields with some coherence reproduce the observed smoothness of the profiles better than randomly moving clumps.

There has been considerable discussion over the last decade concerning the correlation of the luminosity of ^{12}CO J = 1–0 with the molecular mass of a cloud (e.g. Solomon et al 1987). Wolfire et al (1993) have self-consistently calculated the temperature and CO abundance as a function of position in clouds of various mass in order to predict the ^{12}CO J = 1–0 luminosity. The PDR models match the observed correlation well, largely independent of G_0 in the range of $0.1 \lesssim G_0 \lesssim 10^3$. Sodroski et al (1995) present empirical evidence

that the correlation factor changes by a factor of 20 when one compares the Galactic center with Galactic molecular clouds at 13 kpc. This change is hard to reconcile with the Wolfire et al model, although the metallicity gradient may enhance the factor gradient in this case.

5.2 *X-Ray Dissociation Regions (XDRs)*

Completely analogous to PDRs, XDRs can be defined as predominantly neutral gas in which X rays dominate the chemistry and/or the heating (see Maloney et al 1996, Sternberg et al 1997 for review). X rays can dominate the gas heating by photoionizing atoms and molecules and depositing a significant fraction of the primary and secondary electron energy into heat. X rays can also dominate much of the chemistry through the collisional dissociation and ionization of species by secondary electrons and through the photodissociation and photoionization by FUV photons produced via excitation of H and H_2 in collisions with secondary electrons. Molecular gas can be exposed to X rays in a wide range of astrophysical environments: in AGNs, near supernova remnants or fast shocks, around PNe with very hot central stars, and in molecular clouds with embedded X-ray sources such as massive stars, young stellar objects with X-ray active chromospheres, X-ray binaries, or accreting compact objects.

Early work focused on specialized aspects of the chemistry, thermal balance, and H_2 excitation in XDRs (Krolik & Kallman 1983, Lepp & McCray 1983, Krolik & Lepp 1989, Draine & Woods 1990, 1991, Voit 1991, Wolfire & Königl 1993, Gredel & Dalgarno 1995, Lepp & Dalgarno 1996, Yan & Dalgarno 1997) Recently, Maloney et al (1996) have done a comprehensive parameter study of equilibrium XDRs, studying the density range $n = 10^3$–10^5 cm^{-3} and X-ray ionization rates that range from cosmic ray ionization rates to rates that nearly completely ionize the gas. They derive XDR spectra and show, for example, that [Fe II] 1.26 and 1.64 μm and H_2 2 μm emission observed in Seyfert nuclei can originate in XDRs, and not in shocks as had been previously speculated (e.g. Moorwood & Oliva 1990, 1994, Mouri et al 1990a,b). Neufeld et al (1994) and Neufeld & Maloney (1995) applied these XDR models to the higher densities ($n \sim 10^9$ cm^{-3}) and X-ray fluxes incident upon the ∼0.1–1 pc disks or tori that orbit the central engines of AGN. They showed that luminous water maser emission is characteristically produced under these conditions, explaining the origin of the H_2O megamaser sources. All of the 16 megamasers now known are associated with active galactic nuclei (see Maloney 1997, and references therein).

5.3 *The Starburst Nucleus of M82*

Wolfire et al (1990) show how theoretical PDR models can be compared with IR and ^{12}CO observations to derive numerous interesting average physical

parameters that describe the ISM in the central ∼1 kpc of relatively nearby IR-bright galaxies. Results have been obtained for M82 by Watson et al (1984), Crawford et al (1985), Lugten et al (1986), Wolfire et al (1990), Harris et al (1991), Schilke et al (1993), White et al (1994), and Lord et al (1996). The derived average gas density in the PDR clouds in the central 500 pc of M82, a relatively typical bright starburst region, is $\sim 10^4$ cm^{-3}, and the average incident FUV flux $G_0 \sim 10^3$ (Table 1). The atomic (C^+) temperatures are ∼250 K, and the mass in the C^+ component is very significant, ∼10% of the total gas mass. The gas-phase silicon abundances are high, $x_{Si} \sim 1.5 \times 10^{-5}$ (∼0.5 solar), which may result from supernova shock destruction of silicate grains. A significant amount of [Si II] emission, and to a lesser extent [C II], may originate from relatively diffuse H II regions (Carral et al 1994, Lord et al 1996). The derived number of clouds and their sizes are surprising; there are numerous ($N \sim 3 \times 10^5$) small ($R \lesssim 1$ pc) clouds present. These "clouds" are individual entities in the sense that they cannot shadow each other from the FUV flux. Nevertheless, they may be clustered together in sheets or filaments. The average conditions in the central 500 pc of M82 are far different from the average ISM conditions in the solar vicinity: The thermal pressures, densities, and FUV fields are higher by factors on the order of 10^3, 10^2, and 10^3 respectively. They resemble the conditions found in PDRs associated with Galactic reflection nebulae such as NGC 2023.

5.4 *FUV Regulation of Star Formation in Galaxies*

McKee (1989) and Bertoldi & McKee (1996) explain the observed constancy of A_v (∼7.5) in molecular clouds and the regulation of low-mass star formation with a PDR model. They assume that the rate of low-mass star formation is governed by ambipolar diffusion (cf Shu et al 1987) and that newly formed stars inject mechanical energy into the cloud, which supports the cloud against gravitational collapse. The ambipolar diffusion rate is set by the ionization fraction, which depends on the dust shielding of the FUV flux. In the model, the star formation rate increases as the cloud collapses, A_v increases, the FUV-produced ionization level decreases, and the ambipolar diffusion rate increases. However, the cloud collapse is halted as the increased star formation injects turbulent energy. Equilibrium is achieved when $A_v \sim 7.5$. The external FUV flux, in controlling the ionization fraction in most of the cloud, regulates the low-mass star formation rate and the cloud column density.

Parravano (1987, 1988, 1989) proposes that a global feedback mechanism exists in galaxies whereby the galaxy-wide rate of high-mass star formation is also regulated by the interaction of the FUV with the neutral gas. Non–gravitationally bound neutral gas may exist in two phases (cold, ∼100 K, and warm, $\sim 10^4$ K) in a galaxy, if the ISM pressure lies in a critical range

$P_{min} < P < P_{max}$ (Field et al 1969). For pressures $P < P_{min}$, only the warm diffuse phase exists. Parravano makes two assumptions in his modeling: (*a*) grain photoelectric heating dominates both phases so that P_{min} monotonically increases with G_0, and (*b*) molecular star-forming clouds grow out of the cold phase (e.g. out of the coalescence of cold phase clouds). If the pressure P of the ISM is greater than P_{min}, then the cold phase exists, molecular clouds grow, OB stars form, G_0 increases, and P_{min} rises. If P_{min} exceeds P, however, then the cold phase no longer exists, star formation drops, and G_0 and P_{min} both decrease. Thus, the global OB star formation rate is regulated so that $P_{min} \sim P$ in galaxies. Parravano (1988, 1989) offers some observational support of this prediction in external galaxies. Parravano & Mantilla (1991) discuss the radial dependence of the state of the ISM in the Galaxy when both the McKee (1989) and the above self-regulation mechanism are operative.

6. CONCLUDING REMARKS

PDRs emit much of the IR radiation (line and continuum) in galaxies. Most of the mass of the gas and dust in the Galaxy resides in PDRs and is significantly affected, either via chemistry or heating, by the FUV flux. Much of the gas is heated by the grain photoelectric heating mechanism. The spectra from PDRs is characterized by luminosity ratios $(L_{CII} + L_{OI})/L_{IR} \sim 10^{-3}$–$10^{-2}$. PDRs are the origin of much of the FIR dust continuum, the near- and mid-IR PAH emission features, and the [C II] 158 μm, [O I] 63,145 μm, [Si II] 35 μm, [C I] 370,609 μm, low J CO, and C I recombination radiation. PDRs also emit significant H_2 rovibrational emission. In regions such as Orion, NGC 2023, NGC 7027, the Galactic center, and the nucleus of M82, the spectra diagnose physical conditions such as the gas density, the temperature, the clumpiness of the clouds, the FUV radiation field, and the elemental abundances. New models of X-ray illuminated molecular clouds may explain near-IR observations of Seyfert nuclei without invoking star formation. PDR models explain the observed correlations of [C II] 158 μm emission with ^{12}CO J = 1–0 emission, of $(L_{CII} + L_{OI})$ with L_{IR}, and of ^{12}CO J = 1–0 with H_2 mass. The FUV flux in PDRs may regulate low- and high-mass star formation and the column density of gravitationally bound star-forming molecular clouds.

ACKNOWLEDGMENTS

We would like to acknowledge useful comments on early versions of this paper by D Jaffe, A Sternberg, H Störzer, and J Stutzki. This research was supported in part by the NASA Astrophysical Theory Program, which funds the Center for Star Formation Studies, a consortium of researchers from NASA Ames,

University of California at Berkeley, and University of California at Santa Cruz.

Literature Cited

Abgrall H, LeBourlot J, Pineau des Forêts G, Roueff E, Flower D, et al. 1992. *Astron. Astrophys.* 253:525–36

Allamandola LJ, Tielens AGGM, Barker JR. 1989. *Ap. J. Suppl.* 71:733–75

Andersson B-G, Wannier PG. 1993. *Ap. J.* 402: 585–92

Bakes ELO, Tielens AGGM. 1994. *Ap. J.* 427: 822–38

Bally J, Langer WD. 1982. *Ap. J.* 255:143–48

Becklin EE, Gatley I, Werner MW. 1982. *Ap. J.* 258:135–42

Bennett CL, Fixsen DJ, Hinshaw G, Mather JC, Moseley SH, et al. 1994. *Ap. J.* 434:587–98

Bertoldi F, Draine BT. 1996. *Ap. J.* 458:222–32

Bertoldi F, McKee C. 1996. In *Amazing Light*, ed. RY Chiao, pp. 41–53. New York: Springer-Verlag

Black JH, Dalgarno A. 1976. *Ap. J.* 203:132–42

Black JH, Dalgarno A. 1977. *Ap. J. Suppl.* 34:405–23

Black JH, van Dishoeck EF. 1987. *Ap. J.* 322: 412–49

Bobrowsky M, Zipoy DM. 1989. *Ap. J.* 347: 307–24

Boissé P. 1990. *Astron. Astrophys*. 228:483–502

Boland W, de Jong T. 1982. *Ap. J.* 261:110–14

Boreiko RT, Betz AL. 1991. *Ap. J.* 369:382–94

Boreiko RT, Betz AL. 1996a. *Ap. J. Lett.* 464:L83–L86

Boreiko RT, Betz AL. 1996b. *Ap. J. Lett.* 467:L113–16

Burke JR, Hollenbach DJ. 1983. *Ap. J.* 265:223–34

Burton M. 1992. *Aust. J. Phys.* 45:463–85

Burton M, Bulmer M, Moorhouse A, Geballe TR, Brand PWJL. 1992a. *MNRAS* 257:1P–6P

Burton M, Geballe TR, Brand PWJL, Moorhouse A. 1990a. *Ap. J.* 352:625–29

Burton M, Hollenbach D, Tielens AGGM. 1990b. *Ap. J.* 365:620–39

Burton M, Hollenbach D, Tielens AGGM. 1992b. *Ap. J.* 399:563–72

Burton M, Puxley P. 1990. In *The Interstellar Medium in External Galaxies*, ed. DJ Hollenbach, HA Thronson, pp. 238–40. Washington, DC: NASA Conf. Publ. 3084

Cardelli JA, Clayton GC, Mathis JS. 1989. *Ap. J.* 345:245–56

Cardelli JA, Meyer DM, Jura M, Savage BD. 1996. *Ap. J.* 467:334–40

Carral P, Hollenbach DJ, Lord SD, Colgan SWJ, Haas MR, et al. 1994. *Ap. J.* 423:223–36

Chieze JP, Pineau des Forêts G. 1989. *Astron. Astrophys.* 221:89–94

Chieze JP, Pineau des Forêts G. 1990. In *Physical Processes in Fragmentation and Star Formation*, ed. R Capuzzo-Dolcetta, C Chiosi, A DiFazio, pp. 17–25. Dordrecht: Kluwer

Chieze JP, Pineau des Forêts G, Herbst E. 1991. *Ap. J.* 373:110–22

Chrysostomou A, Brand PWJL, Burton MG, Moorhouse A. 1992. *MNRAS* 256:528–34

Chrysostomou A, Brand PWJL, Burton MG, Moorhouse A. 1993. *MNRAS* 265:329–39

Churchwell E, Felli M, Wood DOS, Massi M. 1987. *Ap. J.* 321:516–29

Clavel J, Viala YP, Bel N. 1978. *Astron. Astrophys.* 65:435–48

Cohen M, Allamandola L, Tielens AGGM, Bregman J, Simpson JP, et al. 1985. *Ap. J.* 302:737–49

Crawford MK, Genzel R, Townes CH, Watson DM. 1985. *Ap. J.* 291:755–71

Dalgarno A. 1985. In *Molecular Astrophysics*, ed. GHF Diercksen, WF Huebner, PW Langhof, pp. 281–94. Dordrecht: Reidel

Danks AC, Federman SR, Lambert DL. 1984. *Astron. Astrophys.* 130:62–66

deJong T. 1977. *Astron. Astrophys.* 55:137–45

deJong T, Dalgarno A, Boland W. 1980. *Astron. Astrophys.* 91:68–84

d'Hendecourt L, Léger A. 1987. *Astron. Astrophys.* 180:L9–L12

Diaz RI, Franco J, Shore SN. 1996. *Bull. Am. Astron. Soc.* 188:4010

Dinerstein HL. 1991. *PASP* 103:861–64

Dinerstein HL. 1995. In *Asymmetrical Planetary Nebulae*, ed. N Soker, A Harpaz, pp. 35–54. New York: Am. Inst. Phys.

Draine BT. 1978. *Ap. J. Suppl.* 36:595–619

Draine BT, Bertoldi F. 1996. *Ap. J.* 468:269–89

Draine BT, Lee HM. 1984. *Ap. J.* 285:89–108

Draine BT, Woods DT. 1990. *Ap. J.* 363:464–79

Draine BT, Woods DT. 1991. *Ap. J.* 383: 621–38

Eidelsberg MH, Benayoun JJ, Viala YP, Rostas F, Smith PL, et al. 1992. *Astron. Astrophys.* 265:839–42

Escalante V, Sternberg A, Dalgarno A. 1991. *Ap. J.* 375:630–34
Falgarone E, Lis DC, Phillips TG, Pouquet A, Porter DH, et al. 1994. *Ap. J.* 436:728–40
Falgarone E, Phillips TG. 1996. *Ap. J.* 472:191–204
Falgarone E, Pineau des Forêts G, Roueff E. 1995. *Astron. Astrophys.* 300:870–80
Federman SR, Danks AC, Lambert DL. 1984. *Ap. J.* 287:219–27
Federman SR, Glassgold AE, Jenkins EB, Shaya EJ. 1980. *Ap. J.* 242:545–59
Federman SR, Glassgold AE, Kwan J. 1979. *Ap. J.* 227:466–73
Federman SR, Huntress WT. 1989. *Ap. J.* 338:140–46
Federman SR, Strom CJ, Lambert DL, Cardelli JA, Smith VV, et al. 1994. *Ap. J.* 424:772–92
Field GB, Goldsmith DW, Habing HJ. 1969. *Ap. J. Lett.* 155:L149–52
Field GB, Somerville WB, Dressler K. 1966. *Annu. Rev. Astron. Astrophys.* 4:207–44
Flower DR, LeBourlot J, Pineau des Forêts G, Roueff E. 1994. *Astron. Astrophys.* 282:225–32
Fuente A, Martín-Pintado J, Cernicharo J, Bachiller R. 1993. *Astron. Astrophys.* 276:473–88
Fuente A, Martín-Pintado J, Gaume R. 1995. *Ap. J. Lett.* 442:L33–L36
Fuente A, Rodriguez-Franco A, Martín-Pintado J. 1996. *Astron. Astrophys.* 312:599–609
Gardiner WC. 1977. *Acc. Chem. Res.* 10:326–31
Gatley I, Hasegawa T, Suzuki H, Garden R, Brand P, et al. 1987. *Ap. J. Lett.* 318:L73–L76
Genzel R. 1991. In *The Physics of Star Formation and Early Stellar Evolution*, ed. C Lada, N Kylafis, pp. 155–219. Dordrecht: Kluwer
Genzel R. 1992. In *The Galactic Interstellar Medium: Saas Fe Lectures 1991*, ed. W Burton, R Genzel, BG Elmegreen, pp. 1–85. New York: Springer-Verlag
Genzel R, Harris AI, Jaffe DT, Stutzki J. 1988. *Ap. J.* 332:1049–57
Genzel R, Harris AI, Stutzki J. 1989. In *Infrared Spectroscopy in Astronomy, ESA SP–290*, ed. M Kessler, pp. 115–32. Noordwijk: Eur. Space Agency Publ.
Genzel R, Hollenbach D, Townes CH. 1994. *Rep. Prog. Phys.* 57:417–79
Genzel R, Stacey GJ, Harris AI, Townes CH, Geis N, et al. 1990. *Ap. J.* 356:160–73
Genzel R, Watson DM, Crawford MK, Townes CH. 1985. *Ap. J.* 297:766–86
Genzel R, Watson DM, Townes CH, Dinerstein HL, Hollenbach DJ, et al. 1984. *Ap. J.* 276:551–59
Gerola H, Glassgold AE. 1978. *Ap. J. Suppl.* 37:1–31
Gierens K, Stutzki J, Winnewisser G. 1992. *Astron. Astrophys.* 259:271–82
Glassgold AE. 1996. *Annu. Rev. Astron. Astrophys.* 34:241–78
Glassgold AE, Huggins PJ, Langer WD. 1985. *Ap. J.* 290:615–26
Glassgold AE, Langer WD. 1974. *Ap. J.* 193: 73–91
Glassgold AE, Langer WD. 1975. *Ap. J.* 197: 347–50
Glassgold AE, Langer WD. 1976. *Ap. J.* 206: 85–99
Goldshmidt O, Sternberg A. 1995. *Ap. J.* 439: 256–63
Graf P, Herter T, Gull GE, Houck JR. 1988. *Ap. J.* 330:803–8
Graf UU, Eckart A, Genzel R, Harris AI, Poglitsch A, et al. 1993. *Ap. J.* 405:249–67
Graham JR, Serabyn E, Herbst TM, Mathews K, Neugebauer G, et al. 1993. *Astron. J.* 105:250–57
Gredel R, Dalgarno A. 1995. *Ap. J.* 446:852–59
Gussie GT, Taylor AR, Dewdney PE, Roger RS. 1995. *MNRAS* 273:790–800
Güsten R, Fiebig D. 1988. *Astron. Astrophys.* 204:253–62
Habing HJ. 1968. *Bull. Astron. Inst. Netherlands* 19:421–32
Harris AI, Jaffe DT, Silber M, Genzel R. 1985. *Ap. J. Lett.* 294:L93–L96
Harris AI, Hill RE, Stutzki J, Graf UU, Russell APG, et al. 1991. *Ap. J. Lett.* 382:L75–L78
Hartquist TW, Menten KM, Lepp S, Dalgarno A. 1995. *MNRAS* 272:184–88
Hartquist T, Sternberg A. 1991. *MNRAS* 248:48–51
Hasegawa T, Gatley I, Garden RP, Brand P, Ohishi M, et al. 1987. *Ap. J. Lett.* 318:L77–L80
Hayashi M, Hasegawa T, Gatley I, Garden R, Kaifu N. 1985. *MNRAS* 215:31P–36P
Heck EL, Flower DR, LeBourlot J, Pineau des Forêts G, Roueff E. 1992. *MNRAS* 258:377–83
Hegmann M, Kegel WH. 1996. *MNRAS* 283:167–73
Herbst E, Leung CM. 1989. *Ap. J. Suppl.* 69:271–99
Herrmann F, Madden SC, Nikola T, Poglitsch A, Timmermann R, et al. 1997. *Ap. J.* In press
Herter T, Gull GE, Megeath ST, Rowlands N, Houck JR. 1989. *Ap. J.* 342:696–702
Herter T, Houck JR, Graf P, Gull GE. 1986. *Ap. J. Lett.* 309:L13–L16
Hill JK, Hollenbach DJ. 1978. *Ap. J.* 225:390–404
Hippelein HH, Münch G. 1989. *Astron. Astrophys.* 213:323–32
Hobson MP, Jenness T, Padman R, Scott PF. 1994. *MNRAS* 266:972–82

Hobson MP, Scheuer PAG. 1993. *MNRAS* 264:145–60
Hogerheijde MR, Jansen DJ, Van Dishoeck EF. 1995. *Astron. Astrophys.* 294:792–810
Hollenbach DJ. 1988. *Astrophys. Lett. Commun.* 26:191–206
Hollenbach DJ. 1990. In *The Evolution of the Interstellar Medium*, ed. L Blitz, pp. 167–82. San Francisco: Astron. Soc. Pac.
Hollenbach DJ, McKee CH. 1979. *Ap. J. Suppl.* 41:555–92
Hollenbach DJ, McKee CH. 1989. *Ap. J.* 342:306–36
Hollenbach DJ, Natta A. 1995. *Ap. J.* 455:133–44
Hollenbach DJ, Takahashi T, Tielens AGGM. 1991. *Ap. J.* 377:192–209
Hollenbach DJ, Tielens AGGM. 1996. In *The Physics and Chemistry of Interstellar Clouds*, ed. G Winnewisser, GC Pelz, pp. 164–74. Berlin: Springer-Verlag
Hollenbach DJ, Werner M, Salpeter E. 1971. *Ap. J.* 163:165–80
Howe JE, Jaffe DT, Genzel R, Stacey G. 1991. *Ap. J.* 373:158–68
Howe JE, Jaffe DT, Grossman EN, Wall WF, Mangum JG, et al. 1993. *Ap. J.* 410:179–87
Huggins PJ. 1992. In *Mass Loss on the AGB and Beyond*, ed. H Schwarz, pp. 35–54. Noordwijk: Eur. Southern Obs. Publ.
Huggins PJ. 1993. In *Planetary Nebulae, IAU 155*, ed. R Weinberger, A Acker, pp.147–62. Dordrecht: Kluwer
Huggins PJ, Bachiller R, Cox P, Forveille T. 1992. *Ap. J. Lett.* 401:L43–L46
Israel FP, Maloney PR, Geis N, Herrmann F, Madden SC, et al. 1996. *Ap. J.* 465:738–47
Jackson JM, Geis N, Genzel R, Harris AI, Madden S, Poglitsch A, et al. 1993. *Ap. J.* 402:173–84
Jaffe DT, Genzel R, Harris AI, Howe J, Stacey GJ, et al. 1990. *Ap. J.* 353:193–99
Jaffe DT, Howe JE. 1989. *Rev. Mex. Astron. Astrof.* 18:55–63
Jaffe DT, Zhou S, Howe JE, Herrmann F, Madden SC, et al. 1994. *Ap. J.* 436:203–15
Jansen DJ, Spaans M, Hogerheijde MR, van Dishoeck EF. 1995a. *Astron. Astrophys.* 303:541–53
Jansen DJ, van Dishoeck EF, Black JH, Spaans M, Sosin C. 1995b. *Astron. Astrophys.* 302:223–42
Jansen DJ, van Dishoeck EF, Keene J, Boreiko RT, Betz A. 1996. *Astron. Astrophys.* 309:899–906
Jones ME, Barlow SE, Ellison GB, Ferguson EE. 1986. *Chem. Phys. Lett.* 130:218–23
Jura M. 1974. *Ap. J.* 191:375–79
Jura M. 1976. *Ap. J.* 204:12–20
Justtanont K, Tielens AGGM, Skinner CJ, Haas M. 1997. *Ap. J.* In press
Kastner JH, Weintraub DA, Gatley I, Merrill KM, Probst RG. 1996. *Ap. J.* 462:777–85
Keene J. 1995. In *The Physics and Chemistry of Interstellar Molecular Clouds*, ed. G Winnewisser, GC Pelz, pp. 186–94. Berlin: Springer-Verlag
Keene J, Blake GA, Phillips TG, Huggins PJ, Beichman CA. 1985. *Ap. J.* 299:967–80
Keene J, Lis DC, Phillips TG, Schilke P. 1997. In *Molecules in Astrophysics: Probes & Processes*, ed. E van Dishoeck. Dordrecht: Kluwer. In press
Köster B, Störzer H, Stutzki J, Sternberg A. 1994. *Astron. Astrophys.* 284:545–58
Kramer C, Stutzki J, Winnewisser G. 1996. *Astron. Astrophys.* 307:915–35
Krolik JH, Kallman TR. 1983. *Ap. J.* 267:610–24
Krolik JH, Lepp S. 1989. *Ap. J.* 347:179–85
Langer WD. 1976. *Ap. J.* 206:699–712
Latter WB, Kelly DM, Hora JL, Deutsch LK. 1995. *Ap. J. Suppl.* 100:159–67
Latter WB, Walker CK, Maloney PR. 1993. *Ap. J. Lett.* 419:L97–L100
Leach S. 1987. In *Polycyclic Aromatic Hydrocarbons and Astrophysics*, ed. A Léger, L d'Hendecourt, N Boccara, pp. 99–127. Dordrecht: Reidel
LeBourlot J, Pineau des Forêts G, Roueff E, Flower DR. 1993. *Astron. Astrophys.* 267: 233–54
Lee H-H, Herbst E, Pineau des Forêts G, Roueff E, LeBourlot J. 1996. *Astron. Astrophys.* 311:690–707
Lee KT, Bowman JM, Wagner AF, Schatz GC. 1982. *J. Chem. Phys.* 76:3583–96
Léger A, Puget JL. 1989. *Annu. Rev. Astron. Astrophys.* 27:161–98
Lemaire JL, Field D, Gerin M, Leach S, Pineau des Forêts G, et al. 1996. *Astron. Astrophys.* 308:895–907
Lepp S, Dalgarno A. 1988. *Ap. J.* 335:769–73
Lepp S, Dalgarno A. 1996. *Astron. Astrophys.* 306:L21–L24
Lepp S, McCray R. 1983. *Ap. J.* 269:560–67
Light GC. 1978. *J. Chem. Phys.* 68:2831–43
Lis DC, Schilke P, Keene J. 1997. In *CO: 25 Years of Millimeter Wave Spectroscopy*, ed. WB Latter, SJE Radford, PR Jewell, JG Mangum, J Bally. Dordrecht: Kluwer. In press
London R. 1978. *Ap. J.* 225:405–16
Lord SD, Hollenbach DJ, Haas MR, Rubin RH, Colgan SWJ, et al. 1996. *Ap. J.* 465:703–16
Lugten JB, Genzel R, Crawford MK, Townes CH. 1986. *Ap. J.* 306:691–702
Luhman ML, Jaffe DT. 1996. *Ap. J.* 463:191–204
Luhman ML, Jaffe DT, Keller LD, Pak S. 1994. *Ap. J. Lett.* 436:L185–88

Luhman ML, Jaffe DT, Sternberg A, Herrmann F, Poglitsch A. 1997. *Ap. J.* In press
Maloney P. 1997. In *Accretion Phenomena and Related Outflows*, ed. D Wickramasinghe, L Ferrario, G Bicknell. San Francisco: Astron. Soc. Pac. In press
Maloney P, Hollenbach D, Tielens AGGM. 1996. *Ap. J.* 466:561–84
Martin PG, Mandy ME. 1995. *Ap. J.* 455:L89–L92
Martin PG, Schwarz DH, Mandy ME. 1996. *Ap. J.* 461:265–81
Massi M, Churchwell E, Felli M. 1988. *Astron. Astrophys.* 194:116–24
Mathis JS. 1990. *Annu. Rev. Astron. Astrophys.* 28:37–70
Mathis JS. 1997. In *From Stardust to Planetesimals*, ed. Y Pendleton, AGGM Tielens. San Francisco: Astron. Soc. Pac. In press
Mathis JS, Rumpl W, Nordsieck KH. 1977. *Ap. J.* 217:425–33
Matsuhara H, Nakagawa T, Shibai H, Okuda H, Mizutani T, et al. 1989. *Ap. J.* 339:L69–L70
McKee CF. 1989. *Ap. J.* 345:782–801
McKee CF, Storey JWV, Watson DM, Green S. 1982. *Ap. J.* 259:647–56
Meixner M, Haas MR, Tielens AGGM, Erickson EF, Werner M. 1992. *Ap. J.* 390:499–512
Meixner M, Tielens AGGM. 1993. *Ap. J.* 405:216–28
Melnick G, Gull GE, Harwit M. 1979. *Ap. J.* 227:L29–L33
Minchin NR, White GJ, Padman R. 1993. *Astron. Astrophys.* 277:595–608
Mochizuki K, Nakagawa T, Doi Y, Yui YY, Okuda H, et al. 1994. *Ap. J.* 430:L37–L40
Monteiro T. 1991. *Astron. Astrophys.* 241:L5–L8
Moorwood AFM, Oliva E. 1990. *Astron. Astrophys.* 239:78–84
Moorwood AFM, Oliva E. 1994. *Ap. J.* 429: 602–11
Morris M, Serabyn E. 1996. *Annu. Rev. Astron. Astrophys.* 34:645–701
Mouri H, Kawara K, Taniguchi Y, Nishida M. 1990a. *Ap. J. Lett.* 356:L39–L42
Mouri H, Nishida M, Taniguchi Y, Kawara K. 1990b. *Ap. J.* 360:55–62
Natta A, Walmsley CM, Tielens AGGM. 1994. *Ap. J.* 428:209–18
Nelson RP, Langer WD. 1997. *Ap. J.* In press
Neufeld DA, Maloney PR. 1995. *Ap. J.* 447:L17–L20
Neufeld DA, Maloney PR, Conger S. 1994. *Ap. J.* 436:L127–30
Neufeld DA, Spaans M. 1996. *Ap. J.* 473:894–902
O'Dell CR, Wen Z, Hu X. 1993. *Ap. J.* 410:696–700
Parmar PS, Lacy JH, Achtermann JM. 1991. *Ap. J.* 372:L25–L28
Parravano A. 1987. In *Supernova Remnants and the ISM, IAU 101*, ed. RS Roger, TL Landecker, pp. 513–18. Cambridge: Cambridge Univ. Press
Parravano A. 1988. *Astron. Astrophys.* 205:71–76
Parravano A. 1989. *Ap. J.* 347:812–16
Parravano A, Mantilla JCh. 1991. *Astron. Astrophys.* 250:70–83
Phillips TG, Huggins PJ. 1981. *Ap. J.* 251:533–40
Plume R, Jaffe DT, Keene J. 1994. *Ap. J.* 425:L49–L52
Poglitsch A, Stacey GJ, Geis N, Haggerty M, Jackson J, et al. 1991. *Ap. J. Lett.* 374:L33–L36
Poglitsch A, Krabbe A, Madden SC, Nikola T, Geis N, et al. 1995. *Ap. J.* 454:293–306
Prasad SS, Heere KR, Tarafdar SP. 1991. *Ap. J.* 373:123–36
Prasad SS, Huntress WT. 1980. *Ap. J. Suppl.* 43:1–35
Roberge WG, Dalgarno A, Flannery BP. 1981. *Ap. J.* 243:817–26
Roberge WG, Jones D, Lepp S, Dalgarno A. 1991. *Ap. J. Suppl.* 77:287–97
Roger RS, Dewdney PE. 1992. *Ap. J.* 385:536–60
Rubio M, Lequeux J, Boulanger F. 1993a. *Astron. Astrophys.* 271:9–17
Rubio M, Lequeux J, Boulanger F, Booth RS, Garay G, et al. 1993b. *Astron. Astrophys.* 271:1–8
Russell RW, Melnick G, Gull GE, Harwit M. 1980. *Ap. J.* 240:L99–L103
Russell RW, Melnick G, Smeyers SD, Kurtz NT, Gosnell TR, et al. 1981. *Ap. J.* 250:L35–L38
Savage BD, Mathis JS. 1979. *Annu. Rev. Astron. Astrophys.* 17:73–111
Schatz GC. 1981. *J. Chem. Phys.* 74:1133–39
Schatz GC, Elgersma H. 1980. *Chem. Phys. Lett.* 73:21–25
Schatz GC, Wagner AF, Walch SP, Bowman JM. 1981. *J. Chem. Phys.* 74:4984–96
Schilke P, Carlstrom JE, Keene J, Phillips TG. 1993. *Ap. J.* 417:L67–L70
Schinke R, Lester WA. 1979. *J. Chem. Phys.* 72:3754–66
Sellgren K, Allamandola LJ, Bregman JD, Werner MW, Wooden DH. 1985. *Ap. J.* 299:416–23
Serabyn E, Keene J, Lis DC, Phillips TG. 1994. *Ap. J.* 424:L95–L98
Shu FH, Adams FC, Lizano S. 1987. *Annu. Rev. Astron. Astrophys.* 25:23–81
Shull JM. 1978. *Ap. J.* 219:877–85
Sodroski TJ, Odegard N, Dwek E, Hauser MG, Franz BA, et al. 1995. *Ap. J.* 452:262–68
Solomon PM, Rivolo AR, Barrett JW, Yahil A. 1987. *Ap. J.* 319:730–41

Spaans M. 1995. *Models of inhomogeneous interstellar clouds.* PhD thesis. University of Leiden, Leiden, The Netherlands
Spaans M. 1996. *Astron. Astrophys.* 307:271–87
Spaans M, Black JH, van Dishoeck EF. 1997. *Ap. J.* In press
Spaans M, Tielens AGGM, van Dishoeck EF, Bakes ELO. 1994. *Ap. J.* 437:270–80
Spaans M, van Dishoeck EF. 1997. *Astron. Astrophys.* In press
Stacey GJ, Geis N, Genzel R, Lugten JB, Poglitsch A, et al. 1991. *Ap. J.* 373:423–44
Stacey GJ, Jaffe DT, Geis N, Genzel R, Harris AI, et al. 1993. *Ap. J.* 404:219–31
Stecher TP, Williams DA. 1967. *Ap. J. Lett.* 149:L29–L32
Steiman-Cameron TY, Haas MR, Tielens AGGM, Burton MG. 1997. *Ap. J.* In press
Sternberg A. 1988. *Ap. J.* 322:400–9
Sternberg A. 1989. *Ap. J.* 347:863–74
Sternberg A. 1990. *Ap. J.* 361:121–31
Sternberg A. 1992. In *Astrochemistry of Cosmic Phenomena*, ed. PD Singh, pp. 329–32. Dordrecht: Kluwer
Sternberg A, Dalgarno A. 1989. *Ap. J.* 338:199–233
Sternberg A, Dalgarno A. 1995. *Ap. J. Suppl* 99:565–607
Sternberg A, Yan M, Dalgarno A. 1997. In *Molecules in Astrophysics: Probes & Processes*, ed. E van Dishoeck. Dordrecht: Kluwer. In press
Storey JWV, Watson DM, Townes CH. 1979. *Ap. J.* 233:109–18
Störzer H, Stutzki J, Sternberg A. 1995. *Astron. Astrophys.* 296:L9–L12
Störzer H, Stutzki J, Sternberg A. 1996. *Astron. Astrophys.* 310:592–98
Störzer H, Stutzki J, Sternberg A. 1997. *Astron. Astrophys.* In press
Stutzki J, Güsten R. 1990. *Ap. J.* 356:513–33
Stutzki J, Stacey GJ, Genzel R, Graf UU, Harris AL, et al. 1990. In *Submillimetre Astronomy*, ed. GD Watt, AS Webster, pp. 269–73. Dordrecht: Kluwer
Stutzki J, Stacey GJ, Genzel R, Harris A, Jaffe D, Lugten J. 1988. *Ap. J.* 332:379–99
Tanaka M, Hasegawa T, Hayashi SS, Brand PWJL, Gatley I. 1989. *Ap. J.* 336:207–11
Tarafdar SP, Prasad SS, Huntress WT, Villere KR, Black DC. 1985. *Ap. J.* 289:220–37
Tauber J, Goldsmith P. 1990. *Ap. J. Lett.* 356:L63–L66
Tauber J, Lis DC, Keene J, Schilke P, Büttgenbach TH. 1995. *Astron. Astrophys.* 297:567–73
Tauber JA, Tielens AGGM, Meixner M, Goldsmith PF. 1994. *Ap. J.* 422:136–52
Tielens AGGM. 1993. In *Planetary Nebulae*, ed. R Weinberger, A Acker, pp.155–62. Dordrecht: Kluwer
Tielens AGGM. 1994. In *Airborne Astronomy Symposium on the Galactic Ecosystem*, ed. MR Haas, JA Davidson, EF Erickson, pp. 3–22. San Francisco: Astron. Soc. Pac.
Tielens AGGM, Hollenbach DJ. 1985a. *Ap. J.* 291:722–46
Tielens AGGM, Hollenbach DJ. 1985b. *Ap. J.* 291:747–54
Tielens AGGM, Hollenbach DJ. 1985c. *ICARUS* 61:40–47
Tielens AGGM, Meixner MM, van der Werf PP, Bregman J, Tauber JA, et al. 1993. *Science* 262:86–89
Timmermann R, Bertoldi F, Wright CM, Drapatz S, Draine BT, et al. 1996. *Astron. Astrophys.* 315:281–85
Turner BE. 1996. *Ap. J.* 461:246–64
Usuda T, Sugai H, Kawabata H, Inoue Y, Kataza H, et al. 1996. *Ap. J.* 464:818–28
van der Werf PP, Stutzki J, Sternberg A, Krabbe A. 1996. *Astron. Astrophys.* 313:633–48
van Dishoeck EF. 1987. In *Astrochemistry*, ed. MS Vardya, SP Tarafdar, pp. 51–65. Dordrecht: Kluwer
van Dishoeck EF. 1988. In *Rate Coefficients in Astrochemistry*, ed. TJ Millar, DA Williams, pp. 49–62. Dordrecht: Kluwer
van Dishoeck EF. 1991. In *Astrochemistry of Cosmic Phenomena*, ed. PD Singh, pp.143–51. Dordrecht: Kluwer
van Dishoeck EF. 1992. In *Infrared Astronomy with ISO*, ed. T Encrenaz, M Kessler, pp. 283–308. New York: Nova
van Dishoeck EF, Black JH. 1986. *Ap. J. Suppl.* 62:109–39
van Dishoeck EF, Black JH. 1988. *Ap. J.* 334: 711–802
van Dishoeck EF, Black JH. 1989. *Ap. J.* 340: 273–97
Verstraete L, Léger A, d'Hendecourt L, Dutuit O, Deforneau D. 1990. *Astron. Astrophys.* 237:436–44
Viala YP. 1986. *Astron. Astrophys. Suppl.* 64:391–437
Viala YP, Letzelter C, Eidelsberg M, Rostas F. 1988. *Astron. Astrophys.* 193:265–72
Voit GM. 1991. *Ap. J.* 377:158–70
Wagner AF, Graff MM. 1987. *Ap. J.* 317:423–31
Watson WD. 1972. *Ap. J.* 176:103–10
Watson D, Genzel R, Townes CH, Werner MW, Storey JWV. 1984. *Ap. J.* 279:L1–L4
White GJ, Ellison B, Claude S, Dent WRF, Matheson PN. 1994. *Astron. Astrophys.* 284:L23–L26
White GJ, Padman R. 1991. *Nature* 354:511–13
White GJ, Sandell G. 1995. *Astron. Astrophys.* 299:179–92

Williams DA, Hartquist TW. 1984. *MNRAS* 210:141–45
Williams DA, Hartquist TW. 1991. *MNRAS* 251:351–55
Willner SP, Soifer BT, Russell RW, Joyce RR, Gillett FC. 1977. *Ap. J.* 217:L121–24
Wolfire M, Hollenbach D, Tielens AGGM. 1993. *Ap. J.* 402:195–215
Wolfire MG, Hollenbach DJ, Tielens AGGM. 1989. *Ap. J.* 344:770–78
Wolfire MG, Königl A. 1993. *Ap. J.* 415:204–17
Wolfire MG, Tielens AGGM, Hollenbach DJ. 1990. *Ap. J.* 358:116–31
Wright EL, Mather JC, Bennett CL, Cheng ES, Shafer RA, et al. 1991. *Ap. J.* 381:200–9
Wyrowski F, Walmsley CM, Natta A, Tielens AGGM. 1997. *Astron. Astrophys.* In press
Xie T, Allen M, Langer WD. 1996. *Ap. J.* 440:674–85
Yan M, Dalgarno A. 1997. *Ap. J.* In press